diversity

MDPI

Article

Tracing Geographic and Molecular Footprints of Copepod Crustaceans Causing Multifocal Purple Spots Syndrome in the Caribbean Sea Fan *Gorgonia ventalina*

Oksana A. Korzhavina [1], Mikhail A. Nikitin [2], Bert W. Hoeksema [3,4], Maickel Armenteros [5,6], James D. Reimer [7,8] and Viatcheslav N. Ivanenko [1,9,*]

[1] Department of Invertebrate Zoology, Faculty of Biology, Lomonosov Moscow State University, Moscow 119992, Russia; korzhavina@mail.bio.msu.ru
[2] Belozersky Institute of Physico-chemical Biology, Lomonosov Moscow State University, Moscow 119992, Russia; nikitin.fbb@gmail.com
[3] Marine Evolution and Ecology Group, Naturalis Biodiversity Center, 2300 RA Leiden, The Netherlands; bert.hoeksema@naturalis.nl
[4] Groningen Institute for Evolutionary Life Sciences, University of Groningen, 9700 CC Groningen, The Netherlands
[5] Center for Marine Research, University of Havana, Havana 11300, Cuba; maickel.armenteros@gmail.com
[6] Unidad Académica Mazatlán, Instituto de Ciencias del Mar y Limnología, Universidad Nacional Autónoma de México, Mazatlán 82040, Mexico
[7] Molecular Invertebrate Systematics and Ecology Laboratory, Faculty of Science, University of the Ryukyus, 1 Senbaru, Nishihara, Okinawa 903-0213, Japan; zoantharia1973@gmail.com
[8] Tropical Biosphere Research Center, University of the Ryukyus, 1 Senbaru, Nishihara, Okinawa 903-0213, Japan
[9] Faculty of Biology, Shenzhen MSU-BIT University, Shenzhen 518115, China
* Correspondence: ivanenko.slava@gmail.com

Abstract: The recent rise in ocean temperatures, accompanied by other environmental changes, has notably increased the occurrence and spread of diseases in Octocorallia, many species of which are integral to shallow tropical and subtropical coral reef ecosystems. This study focuses on the understanding of these diseases, which has been largely limited to symptomatic descriptions, with clear etiological factors identified in only a fraction of cases. A key example is the multifocal purple spots syndrome (MFPS) affecting the common Caribbean octocoral sea fan *Gorgonia ventalina*, linked to the gall-forming copepods of the genus *Sphaerippe*, a member of the widespread family, Lamippidae. The specialized nature of these copepods as endoparasites in octocorals suggests the potential for the discovery of similar diseases across this host spectrum. Our investigation employed four molecular markers to study disease hotspots in Saint Eustatius, Curaçao, northwest and southwest Cuba, and Bonaire. This led to the discovery of a group of copepod species in these varied Caribbean locations. Importantly, these species are morphologically indistinguishable through traditional methods, challenging established taxonomic approaches. The observed diversity of symbionts, despite the host species' genetic uniformity, is likely due to variations in larval dispersal mechanisms. Our phylogenetic analyses confirmed that the Lamippidae copepods belong to the order, Poecilostomatoida (Copepoda), and revealed their sister group relationship with the Anchimolgidae, Rhynchomolgidae, and Xarifiidae clades, known for their symbiotic relationships with scleractinian corals. These results add to our understanding of the evolutionary and ecological interactions of copepods and their hosts, and the diseases that they cause, and are important data in a changing climate.

Keywords: parasites; gorgonian octocorals; integrative taxonomic approach; phylogenetic analysis; Caribbean region; copepod crustaceans; Lamippidae

Citation: Korzhavina, O.A.; Nikitin, M.A.; Hoeksema, B.W.; Armenteros, M.; Reimer, J.D.; Ivanenko, V.N. Tracing Geographic and Molecular Footprints of Copepod Crustaceans Causing Multifocal Purple Spots Syndrome in the Caribbean Sea Fan *Gorgonia ventalina*. *Diversity* **2024**, *16*, 280. https://doi.org/10.3390/d16050280

Academic Editors: Luc Legal and Pamela Hallock

Received: 3 December 2023
Revised: 25 April 2024
Accepted: 25 April 2024
Published: 9 May 2024

1. Introduction

In an era characterized by the relentless advance of global climate change and the ever-escalating impact of anthropogenic pollution, the resilience of marine ecosystems is facing unprecedented challenges. Among the denizens of the oceanic realm, octocorals (Cnidaria, Octocorallia) are becoming increasingly susceptible to an onslaught of novel and potent infectious agents. This heightened vulnerability has manifested in a concerning surge of epidemic outbreaks, accompanied by substantial mass mortalities, with profound repercussions for the diversity and extent of octocoral populations [1–3].

Octocorals, with their intricate ecological roles, stand as keystones in the complex web of life within shallow-water tropical and subtropical coral reef ecosystems. They function as essential contributors to ecosystem productivity and as indispensable havens and sustenance sources for a multitude of invertebrate species interconnected within their holobiont networks. The diminishment in octocoral numbers, however, has left an indelible mark on the overall composition, structural integrity, and functional dynamics of these vital marine ecosystems [1,4–7].

Nowhere is this ecological crisis more evident than in the Caribbean region, a global epicenter of octocoral diversity. Home to approximately 70% of the world's infection-prone octocoral species, this region has borne the brunt of the mounting environmental pressures [1,8–10]. Within the confines of this hotspot, our ecological understanding of the infectious agents, transmission mechanisms, and the holistic impacts of these diseases remains confined to only eight [1]. Of particular note, *Gorgonia ventalina* (Linnaeus, 1758), an endemic Caribbean sea fan [11], exhibits susceptibility to nine of these diseases, distinguishing it as the most disease-prone species among octocorals. The multifocal purple spots syndrome (MFPS) that afflicts *G. ventalina* is particularly enigmatic, as it is incited by gall-forming copepods of the genus *Sphaerippe* Grygier, 1980 within the family, Lamippidae [12–15].

The Lamippidae family, notable for its extensive yet homogenous distribution, contains highly specialized obligate endoparasites, characterized by their highly modified body shapes and remarkable reduction of appendages [13,16–19]. These lamippids find residence within the mesoglea, coenosarcal channels, or galls of octocorals on a nearly global scale with the exclusion of the Indian Ocean, and thrive across an astonishing depth range, spanning from the shallows to bathyal depths of 2258 m [13]. Presently, the scientific community has documented 54 lamippid species, with 115 recorded observations worldwide. However, in the Caribbean region, there have been only 14 findings across eight species [13–15]. It is imperative to acknowledge, however, that a significant portion of lamippid species remains concealed, a consequence of the inherent challenges associated with their detection [19]. This gap in our exploration of lamippid biology and virulence imposes substantial obstacles in our endeavors to model potential epizootic events and formulate effective control measures [20–22].

In light of these pressing ecological concerns, the principal objective of this study was to determine the elusive causative agents responsible for the MFPS in Gorgonia ventalina. Through comprehensive investigation, this research aims to enrich our understanding of the intricate interactions between octocorals and their parasitic copepods. Ultimately, our efforts are aimed at contributing to the preservation and management of octocoral populations, striving to mitigate the dire consequences of the mounting environmental challenges for these vital marine organisms.

2. Material and Methods

2.1. Specimen Collection

Our research involved the collection of 30 octocoral colonies from depths of 1–20 m across 18 different Caribbean reefs and three marine ecoregions [23]. These collections occurred at St. Eustatius (eleven samples in 2015), Curaçao (four samples in 2017), southwest Cuba (four samples in 2019), northwest Cuba (nine samples in 2019), and Bonaire (four samples in 2019) (Table 1, Figure 1). The targeted octocoral colonies were *Gorgonia ventalina* (Alcyonacea: Gorgoniidae), selected through SCUBA diving by V.N. Ivanenko

(V.N.I.) and O.A. Korzhavina (OAK). Underwater photographs of the hosts were taken by V.N.I. (Figures S1–S7), and the colonies were then carefully placed in plastic bags and transported to the surface.

Table 1. Localities (Figure 1), studied specimens, and sequence availability of gall-causing copepod of *Sphaerippe* spp. from *Gorgonia ventalina* in three marine ecoregions: the Greater Antilles (Cuba), the Eastern Caribbean (St. Eustatius) and the Southern Caribbean (Bonaire and Curaçao).

Locality Name	Coordinates	Date of Sampling	Collector(s)	Name of Specimens	Depth, m	Coral	Copepods
Gibraltar, St. Eustatius, (Figure 1, point 1)	17°31′36.5″ N 62°59′57.5″ W	12 June 2015	V.N.I.	Statia15-99	5–20	+	+
Anchor Point North, St. Eustatius (Figure 1, point 2)	17°27′50.0″ N 62°59′15.7″ W	17 June 2015	V.N.I.	Statia15-134 Statia15-135	15–20 15–20	+ +	
Anchor Reef, St. Eustatius (Figure 1, point 3)	17°27′44.8″ N 62°59′07.7″ W	18 June 2015	V.N.I.	Statia15-141 Statia15-142	15.6 15.6	+ +	+ +
English Quarter, St. Eustatius (Figure 1, point 4)	17°30′18.2″ N 62°57′46.3″ W	19 June 2015	V.N.I.	Statia15-146	17.3	+	
Twin Sisters, St. Eustatius (Figure 1, point 5)	17°30′59.6″ N 63°00′10.8″ W	22 June 2015	V.N.I.	Statia15-163	13.8	+	
Blund Shoal, St. Eustatius (Figure 1, point 6)	17°27′52.6″ N 62°58′38.7″ W	26 June 2015	V.N.I.	Statia15-170	5.9		+
Gallows Bay, St. Eustatius (Figure 1, point 7)	17°28′30.3″ N 62°59′10.3″ W	27 June 2015	V.N.I.	Statia15-173 Statia15-174	13.8 2–3	 +	+
Director's Bay, Curaçao, (Figure 1, point 8)	12°03′59″ N 68°51′38″ W	13 June 2017	V.N.I.	Cur17-39	4.1	+	+
Tugboat 2, Curaçao (Figure 1, point 9)	12°04′05″ N, 68°51′44″ W	19 June 2017	V.N.I.	Cur17-81	5.2–5.5	+	
Playa Lagun, Curaçao (Figure 1, point 10)	12°19′02″ N, 69°09′09″ W	20 June 2017	V.N.I.	Cur17-88	4.9	+	
Buoy 1, Curaçao (Figure 1, point 11)	12°07′23″ N, 68°58′14″ W	21 June 2017	V.N.I.	Cur17-96	8.2	+	
Alejo el Moro, Cuba (Figure 1, point 12)	22°06′54.99″ N 81°06′58.96″ W	4 February 2019	V.N.I., O.A.K.	Cuba19-1 Cuba19-2 Cuba19-3	7.0 8.5 4.5	+ + +	+ + +
Punta Perdiz, Cuba (Figure 1, point 13)	22°06′29.65″ N 81°06′49.42″ W	4 February 2019	V.N.I., O.A.K.	Cuba19-5	4.8–5.0	+	+
Coast near Havana University, Cuba (Figure 1, point 14)	23°07′38.75″ N 82°25′21.68″ W	7 February 2019	V.N.I., O.A.K.	Cuba19-21 Cuba19-22 Cuba19-23 Cuba19-25	11.6 8.5 11 8.1–8.2	 + + +	+ + +
El Salado, Cuba (Figure 1, point 15)	23°02′20.33″ N 82°36′18.55″ W	8 February 2019	V.N.I., O.A.K.	Cuba19-27 Cuba19-28 Cuba19-30 Cuba19-32	13.8 10.0 12.6 8.3	+ + +	+ + + +
Red Beryl, Bonaire (Figure 1, point 16)	12°2′49.14″ N 68°16′4.38″ W	28 October 2019	V.N.I.	Bonaire19-28	5	+	+
Red Slave, Bonaire (Figure 1, point 17)	12°1′36.3″ N 68°15′4.74″ W	29 October 2019	V.N.I.	Bonaire19-31	14	+	+
Cai (outside of lagoon), Bonaire (Figure 1, point 18)	12°6′10.98″ N 68°13′19.98″ W	31 October 2019	V.N.I.	Bonaire19-47	11	+	+
Klein Bonaire: South Bay, Bonaire (Figure 1, point 19)	12°9′0.06″ N 68°19′14.04″ W	8 November 2019	V.N.I.	Bonaire19-91	3	+	+

Figure 1. (**a**) Sampling localities are distributed over three marine ecoregions in the Caribbean Sea (details in Table 1): (**b**) Cuba in the Greater Antilles; (**c**) Bonaire and Curaçao in the Southern Caribbean, and (**d**) St. Eustatius in the Eastern Caribbean.

Subsequent examinations of these colonies focused on identifying the presence of purple spots. The spotted tissues were preserved in 96% ethanol for later analyses. These spots were dissected to isolate copepods under a binocular Olympus SZX7 microscope (Olympus, Tokyo, Japan). The copepods were then prepared for morphological examination on glass slides in glycerine or placed in individual tubes for molecular analyses. Additionally, small sections of healthy coral tissue were separately preserved in tubes for DNA identification purposes. To complete the preservation process, bulk coral samples were stored in formalin.

2.2. Morphological Examinations

In the study of copepods and their exuviae (exoskeletons) for light microscopy, post-DNA extraction, we employed the "hanging drop method" using the Olympus CX41RF and Olympus BX 51 microscopes (Olympus, Tokyo, Japan), following the methodologies outlined by Ivanenko and Defaye [24] and Ivanenko et al. [25]. For scanning electron microscopy (SEM), we prepared copepods initially fixed in formalin by washing them in distilled water containing detergent. Subsequently, these specimens underwent a dehydration process involving two or three ethanol washes with increasing concentrations, followed by a transfer to acetone. The specimens were then dried using a critical point dryer (Hitachi HCP-2) (Hitachi, Tokyo, Japan). They were subsequently mounted on aluminum stubs using double-sided sticky tape and gold-coated in an IB-3 WHAT. Imaging was carried out using a JEOL JSM-6380LA (JEOL, Tokyo, Japan) and CamScan-S2 (Cambridge Instruments, Cambridge, UK), resulting in a total of 112 photographs. The electron microscopy was conducted as part of the research at the General Faculty Laboratory of Electron Microscopy, located within the Faculty of Biology at Lomonosov Moscow State University (MSU). These specimens have been added to the collection at the Biological Faculty of MSU for further study and reference.

2.3. DNA Extraction

In our study, we implemented a refined non-destructive DNA extraction methodology, based on the protocol established by Porco et al. [26] and further elaborated in Ivanenko et al. [25]. This process involved individual copepods, secured in 1.5 mL eppendorf tubes, from which 96% ethanol was carefully removed using a pipette with 200 µL tips. Each specimen was then treated with 50 µL of a specially formulated lysis solution (30 mM Tris-HCl, 20 mM EDTA, 1% SDS, 0.1 mg/mL proteinase K), with varying incubation times tailored to the sample's origin: two hours for Curaçao and St. Eustatius, 30 min for Cuba, and a variable 30 to 90 min for Bonaire samples, contingent upon the specimen size. The incubation for samples was attentively monitored, concluding upon the sample's transition to a translucent state. Subsequently, the lysis solution was transferred to new tubes using a pipette equipped with slender 10 µL tips.

For the extraction of DNA from the lysis buffer, a silica-based DNA extraction kit (Diatom DNAprep 100, Isogene, Moscow, Russia) was utilized, following the manufacturer's guidelines for fresh blood samples. The extracted DNA, in volumes of 20–30 µL, was then stored in appropriately labeled sterile tubes at −20 °C for subsequent molecular analyses. Additionally, to preserve the morphological integrity of the copepod exuviae, a mixture of 100 µL of 1:1 ethanol-glycerol was applied.

The coral tissue DNA extraction commenced with the introduction of 300 µL of guanidine buffer, as per the standard instructional guidelines [25]. This was followed by a 2 h incubation at 65 °C, interspersed with vortex shaking at 30 min intervals, paralleling the protocol used for copepod DNA extraction [25]. A set of 91 samples was prepared for molecular study, encompassing 66 samples from lamippid copepods and 25 from their corresponding hosts.

2.4. DNA Amplification and Sequencing

The amplification of genetic material was conducted utilizing an Encyclo Plus PCR kit (Evrogen, Moscow, Russia) on BIO-RAD Dyad and BIO-RAD MJ Mini thermal cyclers. For analyses, three molecular markers were selected: mitochondrial cytochrome c-oxidase subunit I (COI), nuclear transcribed spacer 2 (ITS2) and nuclear ribosomal DNA (18S). These markers were chosen due to the availability of their sequences for most copepod families in existing databases. The COI marker was amplified using the forward copepod-specific primer LCO1490cop3 [25] and the universal reverse primer jgH2198 [27]. ITS2 amplification utilized a pair of copepod-specific primers, 58d-cop and 28-1-cop [25], while universal primers 18d1 (Aleshin, unpublished) and Q39 [28] were employed for the 18S marker. Octocoral DNA markers included ITS2 [29] and msh1 [30], and were selected based on their previous application in octocoral phylogenetic studies and the availability of sequences for the genus *Gorgonia* Linnaeus, totalling 1758 in databases. Details of the primers, amplified region lengths, and annealing temperatures are provided in Tables A1 and A2.

Post-amplification, PCR products were visualized through electrophoresis in 1% or 1.2% agarose gel. For processing, Shrimp Alkaline Phosphatase (SAP) and Exonuclease *I E. coli* enzymes were added to the PCR products, followed by incubation for one hour at 37 °C and subsequent deactivation for 15 min at 85 °C. Sequencing from both ends was performed using a BigDye Terminator reagent kit on ABI 3730 capillary sequencers at Evrogen (Moscow, Russia) following the manufacturer's instructions.

The resulting sequences were assembled and edited using Geneious 8.1 [31] and subsequently stored in the GenBank sequence database (Tables A3 and A4). All sequences underwent verification using the NCBI BLAST tool, and protein-coding sequences (COI) were examined for an open reading frame [32]. We obtained sequences of 18S rDNA (1537–1658 bp) for three *Sphaerippe* samples, COI (618–695 bp) for 56 samples, and ITS2 (441–575 bp) for 59 samples. Additionally, sequences of ITS2 (215–240 bp) were retrieved for 20 *Gorgonia ventalina* samples, and msh1 (781–857 bp) for 21 samples. Sequence alignments were conducted using the MUSCLE algorithm in Geneious for monogenic alignments [33] or MAFFT version 7 [34,35] for concatenated alignments. The phylogenetic trees derived from these alignments are available for review at the TreeBASE online data exchange center.

2.5. DNA Phylogeny and AGBD Analyses

In this detailed phylogenetic study, we conducted Bayesian Analysis (BA) on both individual markers and a combined dataset for copepods, while Maximum Likelihood (ML) analysis was specifically applied to the concatenated alignment of these organisms. Throughout this process, uniform tree-building parameters were employed for all alignments, with the sole variation being the models of nucleotide evolution. These models were selected using MegaX for single-gene alignments and PartitionFinder for the concatenated datasets, in accordance with the established protocols developed by Guindon et al. [36] and Lanfear et al. [37,38].

For the construction of BA phylogenetic trees, we utilized the CIPRES web interface [39]. The procedure included runs over 25 million generations, employing four synchronous Markov Chain Monte Carlo (MCMC) chains and saving every 5000th tree. We excluded the initial 25% of trees from subsequent analyses as 'burn-in'. The convergence of these analyses was monitored using Tracer v1.7.1 [40], with Effective Sample Sizes (ESS) for all parameters exceeding the threshold of 200 to ensure data reliability. Nodal support in the BA trees was assessed based on posterior probabilities, and the ML trees were constructed using the IQ-TREE web application [41], with nodal supports determined via 1000 bootstrap replications [42].

The COI alignment for copepods comprised 56 sequences, predominantly from *Sphaerippe* spp., augmented with lamippid sequences from Australia, while the ITS2 alignment included 59 sequences. Both alignments were modeled using the GTR + G + I model, identified as the most appropriate based on respective selection criteria. The concatenated

alignment, encompassing COI and ITS2 sequences of lamippids, featured 66 sequences for tree construction and 51 sequences for Poisson Tree Processes (PTP) analysis. PartitionFinder was employed to recommend evolutionary models for this alignment's partitions, highlighting the complexity of the genetic data. Additionally, ITS2 and msh1 alignments of *Gorgonia* spp. octocorals included sequences from a range of Caribbean locations and GenBank, representing diverse species within the genus.

Species differentiation was performed using Automated Barcode Gap Detection (ABGD) and Poisson Tree Process (PTP), recognized for their efficacy in DNA taxonomy [43]. The ABGD analysis, executed separately for COI, ITS2, and msh1 markers, identified the genetic distance gaps indicative of interspecific variability. The PTP analysis was applied to the BA trees for both COI, ITS2, and their combined datasets of *Sphaerippe* spp., as well as the msh1 dataset of *Gorgonia* spp., utilizing the bPTP online platform's standard parameters.

2.6. Host Relationships and Geographical Isolation

In our research, we applied the DNAsp program to discern and segregate all the haplotypes within our alignments, effectively removing any repetitive sequences. Additionally, DNAsp was utilized to compute Fu's F parameter to assess the genetic diversity and population dynamics.

For the analysis of haplotypes, we employed the Median Joining method via the PopArt program [44]. Our dataset for this portion of the study consisted of 54 sequences in the COI alignment of *Sphaerippe* spp., and 57 sequences in the ITS2 alignment. The ITS2 alignment for sea fans of the genus *Gorgonia* encompassed 20 of our sequences and an additional three from GenBank. Similarly, the msh1 alignment included 21 sequences of *Gorgonia ventalina* alongside the three sourced from GenBank (Table A5).

The selection of sampling points was derived from expedition data to St. Eustatius (2015), Curaçao (2017), Cuba (2019), and Bonaire (2019), as detailed in a database from a comprehensive review [13]. This approach not only enriched the geographical scope of our study but also facilitated the calculation of statistical parameters, including nucleotide diversity and Tajima's D statistic [45].

2.7. Molecular Phylogenetic Analyses

The phylogenetic positioning of *Sphaerippe* spp. within the copepod clade was ascertained through an analysis of the 18S rDNA alignment. This alignment incorporated 100 copepod sequences from GenBank, which included 53 species from Cyclopoida, 44 from Poecilostomatoida, and three from Misophrioida. Notably, the dataset also contained a sequence from the octocoral *Junceella fragilis* (AY962533.1), which was a lamippid sequence mistakenly categorized under the host name in GenBank. Additionally, four sequences from our samples were included, three of which were from different Caribbean regions representing *Sphaerippe* spp., as well as one lamippid from Lizard Island (Australia) (Table A6). The sequences utilized ranged from 564 to 1866 base pairs in length.

For model selection, the General Time Reversible model with Gamma distribution and Invariant sites (GTR + G + I) was determined as the most suitable using the Akaike Information Criterion with correction (AICc) in Mega X. Bayesian Analysis (BA) was executed with settings as previously mentioned, and the convergence of the results was validated using Tracer v1.7.1 [40]. A Maximum Likelihood (ML) phylogenetic tree was constructed using the standard parameters.

The figures depicting these phylogenetic trees and their associated captions were edited only for clarity using Adobe Photoshop 21.2.9 and CorelDRAW 2021 [46].

3. Results

3.1. Observation of the Purple Galls on Gorgonia ventalina

We conducted a detailed examination of the easily detectable underwater purple galls on the sea fan. These galls predominantly appeared as isolated or, more frequently,

aggregated gall-like growths. These formations, slightly thickened and diverse in structure, were primarily located on the lateral aspects of the stolons or, more typically, at the nodes of the sea fan's reticulate structure, as shown in Figures 2 and S1–S7.

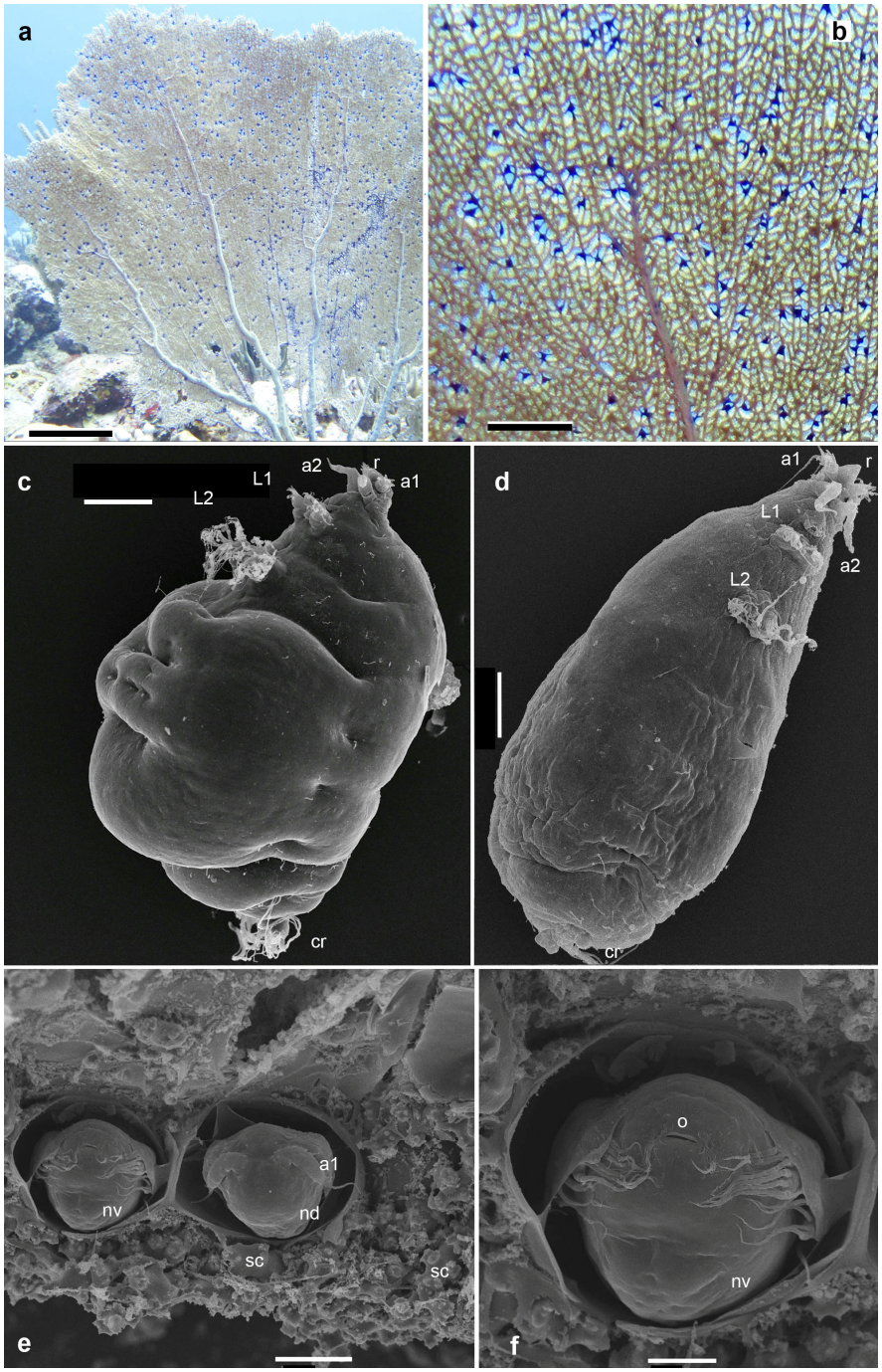

Figure 2. (**a**,**b**) Sea fan *Gorgonia ventalina* with purple galls containing *Sphaerippe* spp. copepods (Lamippidae); (**c**) spherical female of *Sphaerippe* sp.; (**d**) elongated male of *Sphaerippe* sp.; (**e**,**f**) embryonic nauplii in a capsule formed by the sea fan tissues; L1, L2—legs 1–2; a1—antennule, a2 antenna, cr—caudal ramus, o—oral opening, nd—nauplius dorsal view, nv—nauplius, ventral view, r—rostral area, sc—sclerite of the sea fan. Scale bars: a—25 cm, b—5 cm, c–f—100 µm, 50 µm, 50 µm, and 20 µm, respectively.

The dissection of these purple galls devoid of any apparent openings typically detected the presence of one or rarely more chambers containing spheroidal females, typically one

and occasionally two per chamber (Figure 2). These females were often accompanied by a male, and in less frequent cases, two males. Some galls contained elongated copepod stages, which were noticeably smaller than for female and male.

The gall walls formed by the sea fans include numerous microscopic spherical capsules with a diameter of about 0.1 mm. Each capsule contained an embryo covered by a membranous shell. This ranged from early-stage, undifferentiated round embryos to nearly fully formed nauplii, likely on the verge of hatching. The nauplii exhibited typical distinctive features, such as three pairs of anterior appendages, including a uniramous antennule and biramous antennae and mandibles, and had a slit-like oral opening devoid of an overlying labrum (Figure 2).

We uncovered the presence of yellowish, sclerotized structures within galls that housed living copepods and, intriguingly, in some galls live copepods were not observed. These structures are identified as the exoskeletons of mummified copepods along with their spermatophores, seemingly isolated by *Gorgonia ventalina*. All these findings indicate the complex biological and ecological interactions between copepods and their gorgonian hosts.

3.2. Morphological Features of Sphaerippe spp. from the Purple Galls

The females are discernibly different from their male counterparts, primarily in their rounded body morphology accentuated by various projections (Figure 2). These females feature pronounced bulges and folds, dividing the body into distinct sections. Morphological features include a forward-directed conical rostrum, uniramous antennules and antennae, an oral cone, and two pairs of biramous, modified swimming legs located in the anterior portion of the body, complemented by caudal rami. A notable characteristic of the female copepods is the presence of elaborately developed modified setae on the first and second pairs of swimming legs and the caudal rami. These setae split at the base into clusters of long, slender projections. In contrast, the males are characterized by an elongated body shape, with a more extended rostrum. Their modified setae, similar to those of the females, are less developed in comparison.

The analysis of samples collected from different locations, employing both light and scanning electron microscopy, revealed a notable degree of variability among the specimens, even those inhabiting the same locale. The study did not yield any distinct diagnostic morphological features of copepods discernible through molecular methods.

3.3. Interspecies Molecular Diversity

In our comprehensive phylogenetic analyses using Bayesian Analysis (BA) on the COI alignment of Lamippidae copepods, we discerned a separation of Caribbean lamippids into three monophyletic groups. This division was represented by a first clade consisting of samples from Bonaire and Curaçao (both Southern Caribbean), and St. Eustatius (Eastern Caribbean), supported robustly with a probability of 1. The second and third clades, encompassing samples from southwest and northwest Cuba (Greater Antilles), respectively, had supports of 0.76 and 1, respectively (Figure 3). Intriguingly, the northwestern Cuban clade was phylogenetically allied as a sister group to the Eastern + Southern Caribbean clade in the BA framework. Employing the Automatic Barcode Gap Discovery (ABGD) method, we identified three distinct species groups within the COI alignment of *Sphaerippe* spp. corresponding to these three clades, with intraspecific distances ranging from 0.16 to 0.31. The Poisson Tree Processes (PTP) model further corroborated this finding, delineating three potential species in the dataset: *Sphaerippe* sp. 1 from St. Eustatius and Curaçao (support 0.964), *Sphaerippe* sp. 2 from northwest Cuba (support 0.977), and *Sphaerippe* sp. 3 from southwest Cuba (support 0.966).

Similarly, the BA phylogenetic tree, based on the ITS2 alignment of lamippids recovered, is split into Cuban (Greater Antilles) and Eastern + Southern Caribbean monophyletic clades (Figure 4). The ABGD analysis, considering prior intraspecific distances from 0.06 to 0.19, and the PTP model, with supports of 1 and 0.99, respectively, confirmed the existence of two distinct species groups within the ITS2 alignment of *Sphaerippe* spp.

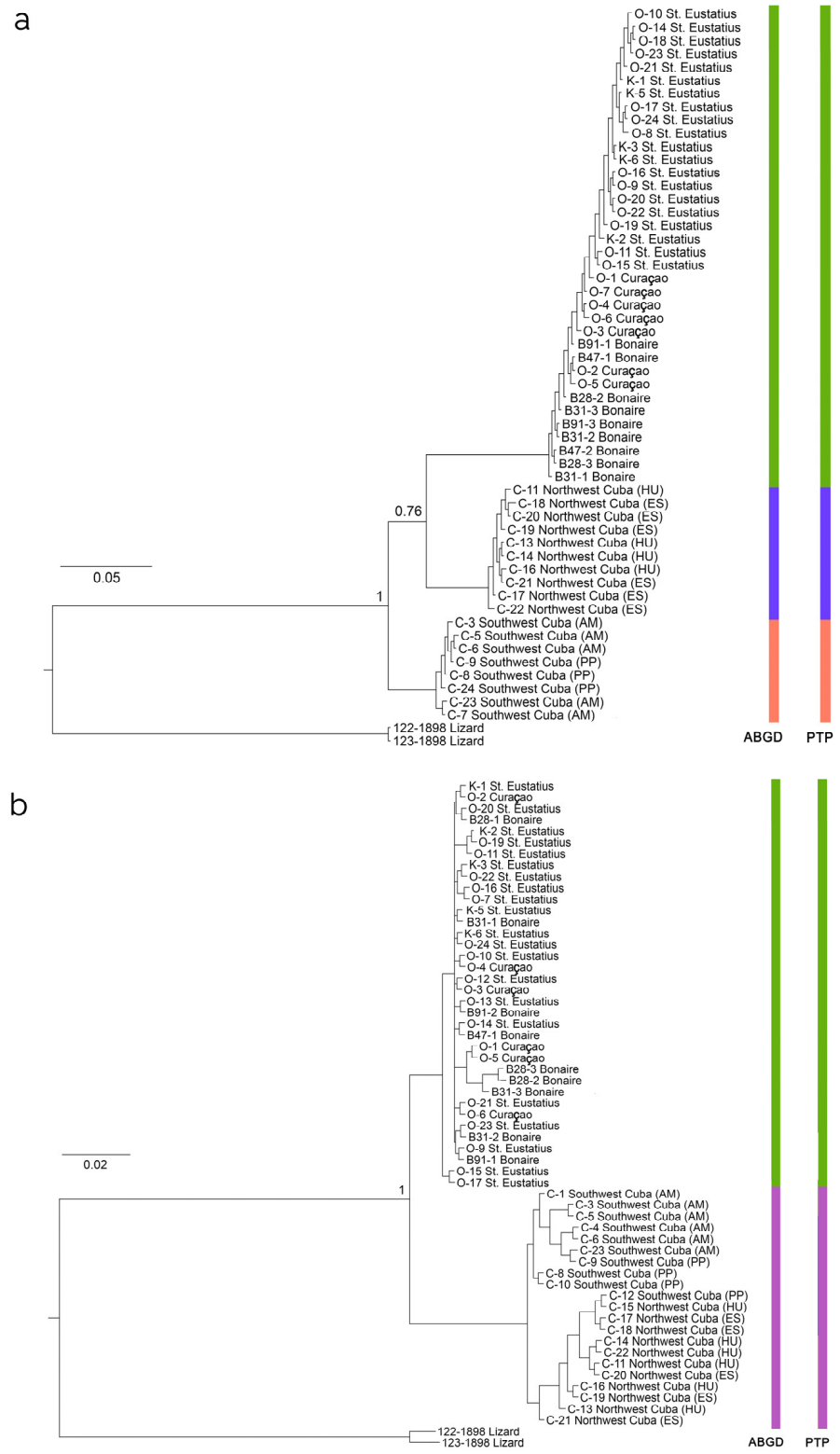

Figure 3. Bayesian inference phylogenetic trees based on COI (**a**) and ITS2 (**b**) alignments of lamippid copepods including *Sphaerippe* spp. The nucleotide evolution model used was GTR + G + I, and the numbers at the nodes represent Bayesian posterior probabilities. Species delimitation results are indicated by color bars on the right. Additional details, including geographic coordinates, are presented in Table 1.

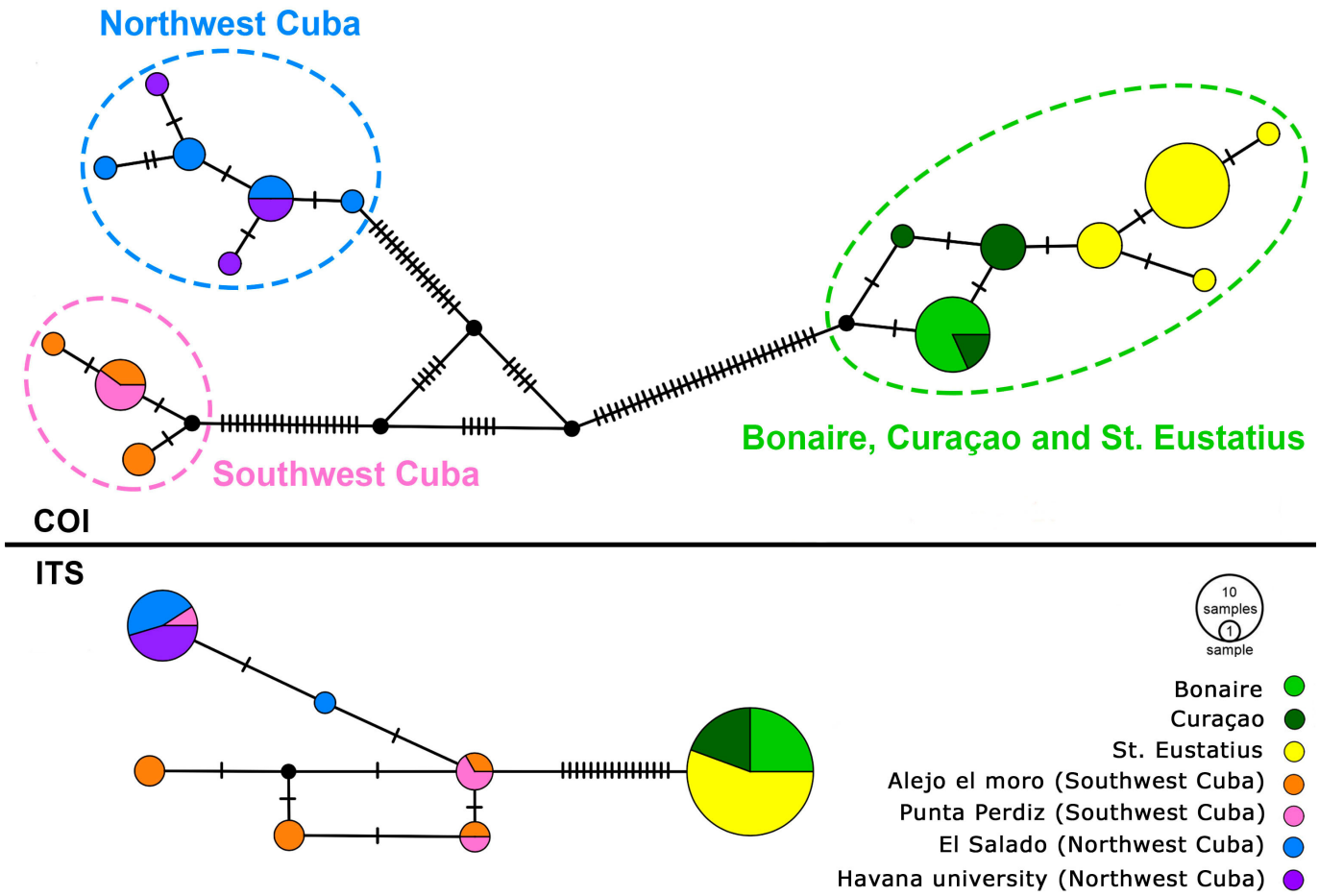

Figure 4. Median-joining networks of COI and ITS2 haplotypes in *Sphaerippe* spp. The representation of haplotype frequency is reflected in the size of the circles, while the notches on connecting lines indicate the number of nucleotide substitutions between haplotypes. Colors distinguish the geographic origins of specimens: yellow signifies individuals collected from St. Eustatius, light and dark green represent Bonaire and Curaçao, orange and pink denote southwest Cuba, and blue and purple are northwest Cuba.

Moreover, the BA and Maximum Likelihood (ML) phylogenetic trees, derived from the copepods' concatenated alignment (COI + ITS2), revealed three distinct monophyletic Caribbean clades (Figure S8). The PTP model applied to this dataset also identified three species: *Sphaerippe* sp. 1 from the islands of St. Eustatius and Curaçao (support 0.847), *Sphaerippe* sp. 2 from southwest Cuba (support 0.84), and *Sphaerippe* sp. 3 from northwest Cuba (support 0.83).

The ITS2 alignment of octocoral samples was characterized by minimal polymorphism, indicating the probable conspecific nature of all samples. The GenBank sequences of *Gorgonia ventalina* and *Gorgonia flabellum* Linnaeus, 1758 revealed only two polymorphic substitutions. The msh1 octocoral alignment presented a similar scenario, with the exception of samples 19–32, which showed nine nucleotide substitutions. Both the ABGD and PTP analyses suggested four species in this dataset: *Pseudopterogorgia bipinnata* (Verrill, 1864), *Gorgonia mariae* Bayer, 1961, the distinct samples 19–32, and a collective group comprising all other samples along with *G. ventalina* and *G. flabellum*. In the PTP analysis, samples 19–32 had a support of 0.79, while the aggregate group, including *G. ventalina* and *G. flabellum*, had a support of 0.64.

3.4. Intraspecific Molecular Diversity

In the phylogenetic investigation, we employed a haploweb constructed from 54 COI sequences of *Sphaerippe* spp., revealing a clear division into a group of two or three species (Figure 4). The analysis of 36 individuals of *Sphaerippe* sp. 1, utilizing the DNAsp program, identified seven distinct haplotypes. These haplotypes are segregated into two geographic clusters, one encompassing the islands of Bonaire with Curaçao in the Southern Caribbean marine ecoregion and the other St. Eustatius in the Eastern Caribbean marine ecoregion. Each neighboring haplotype was differentiated by a single nucleotide substitution, with the most predominant haplotype observed in St. Eustatius, exhibiting a nucleotide distance of n = 1.61. In the dataset of *Sphaerippe* sp. 2, comprising ten specimens, DNAsp analysis delineated six haplotypes, with a nucleotide distance of n = 1.533. Furthermore, the analysis of eight individuals of *Sphaerippe* sp. 3 identified three haplotypes, showing a nucleotide distance of n = 1.107.

The ITS2 haploweb, based on the alignment of 57 sequences of *Sphaerippe* spp., demonstrated divergence into three species (Figure 4). The group of 36 specimens from Bonaire, Curaçao, and St. Eustatius collectively formed a single haplotype, exhibiting identical sequences except for variations in microsatellite repeats. Consequently, nucleotide distances were not computed for this group. In the Cuban *Sphaerippe* dataset, encompassing 21 sequences, the DNAsp program identified six haplotypes with a nucleotide distance of n = 1.867.

Tajima's D and Fu's F statistics [47] for all species of *Sphaerippe* spp. and both DNA markers showed no significant deviations from zero ($p < 0.05$) (Table 2).

Table 2. Results of tests on geographical isolation.

Species of Sample	Localities	Gene	Number of Sequences	Nucleotide Diversity	Tajima's D	Fu's F
Sphaerippe spp.	Bonaire, Curaçao, St. Eustatius	COI	36	0.00264	0.30709	−0.850
Sphaerippe spp.	Northwest Cuba	COI	10	0.00250	−1.49280	−2.563
Sphaerippe spp.	Southwest Cuba	COI	8	0.00168	−0.17740	0.390
Sphaerippe spp.	Bonaire, Curaçao, St. Eustatius	ITS2	36	All sequences identical		
Sphaerippe spp.	Cuba	ITS2	21	0.00635	1.03432	−0.378
Gorgonia ventalina (Linnaeus 1758)	Caribbean region	ITS2	All sequences identical			
Gorgonia ventalina (Linnaeus 1758)	Caribbean region	msh1	25	0.00538	**−1.92207** *	2.449

* **Bold** in the column of Tajima's D statistic means that value is significant.

The haploweb analysis for ITS2 corals of *Gorgonia* Linnaeus, 1758 revealed two haplotypes: one exclusive to *Gorgonia mariae* Bayer, 1961 and the other inclusive of all our samples, *G. flabellum*, and *G. ventalina*. The msh1 haploweb for *G. ventalina* indicated a division into two species, one of which formed two distinct haplotypes (Figure 5), with a nucleotide distance of n = 4. For this species, the values of Tajima's D and Fu's F statistics exhibited significant differences from zero (−1.92207 and 2.499).

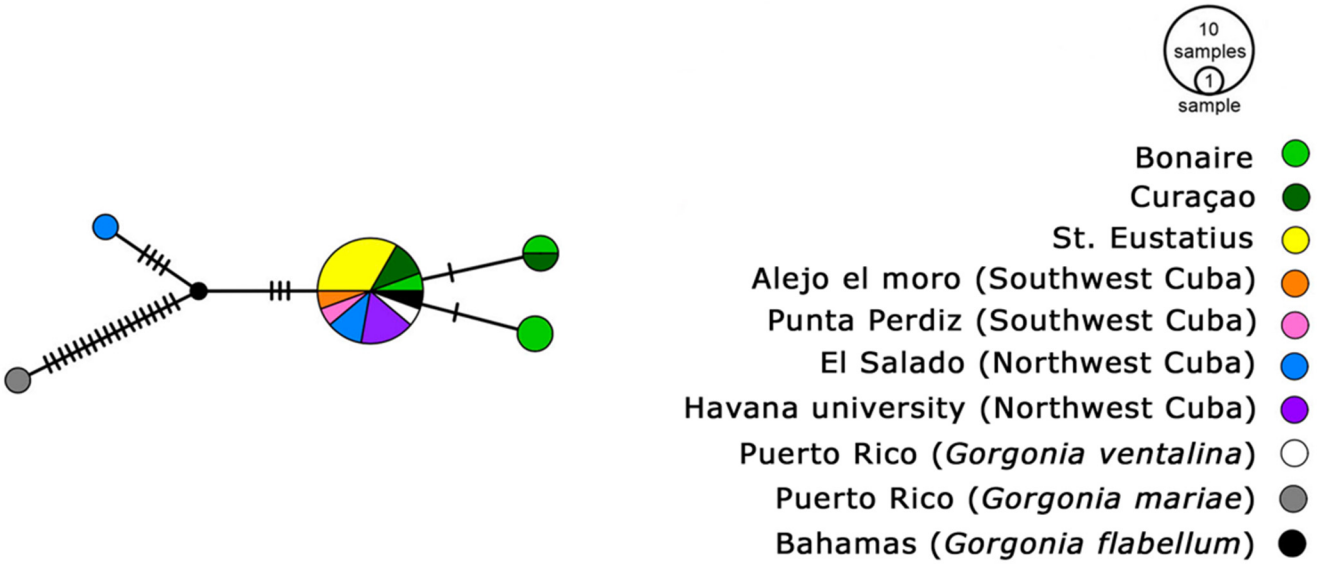

Figure 5. msh1 haplotype diversity in *G. ventalina* across the Caribbean. Circle sizes represent haplotype frequency, notches indicate genetic substitutions. Colors denote geographic origin: yellow for St. Eustatius, light and dark green for Bonaire and Curaçao, orange and pink for southwest Cuba, blue and purple for northwest Cuba, white and gray for Puerto Rico samples (GenBank), and black for Bahamas samples (GenBank).

3.5. Phylogeny Reconstruction

Phylogenetic analyses utilizing Maximum Likelihood (ML) and Bayesian Analysis (BA) based on the 18S alignment robustly positioned the genus *Sphaerippe* within the suborder, Poecilostomatoida (Cyclopoida). These results had 100% support probability (Figures 6, S9 and S10). Within this phylogenetic framework, the Lamippidae family was observed to cluster with the family groups Anchimolgidae, Rhynchomolgidae, Sabelliphilidae Xarifiidae, and, with strong support scores of 100 and 1 in ML and BA trees, respectively. Moreover, the clade comprising Anchimolgidae, Rhynchomolgidae, and Xarifiidae emerged as a sister group to *Sphaerippe* spp., with this relationship receiving high support values of 98 and 0.98 in the ML and BA analyses, respectively.

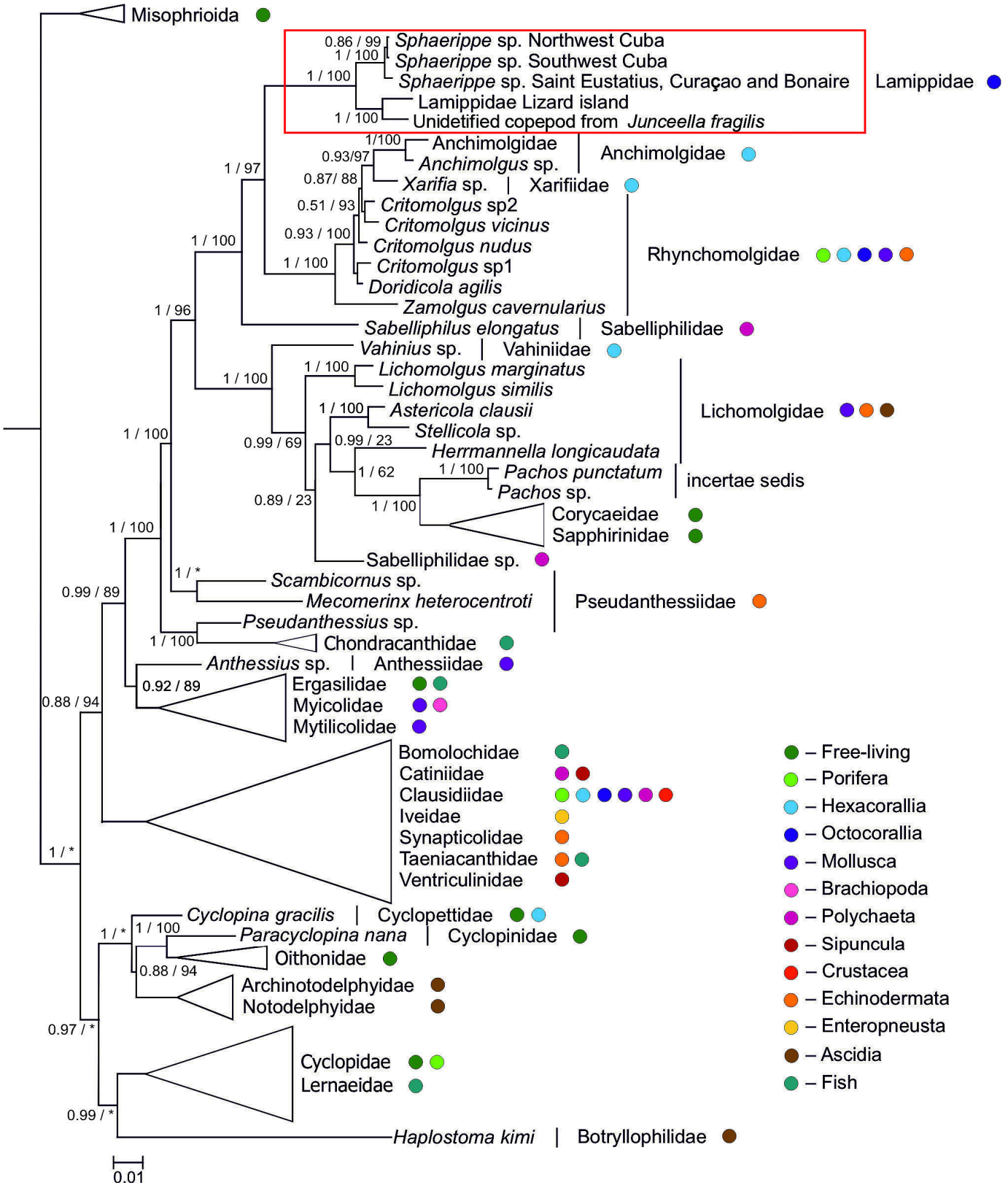

Figure 6. Phylogenetic trees based on 18S alignment using the GTR + G + I nucleotide evolution model. Node numbers indicate posterior probabilities (Bayesian) and bootstrap supports (Maximum Likelihood), with asterisks (*) marking nodes with differing topologies in ML and BA trees. Circle colors represent copepod host taxa, and red frame highlights the position of Lamippidae within the Copepoda.

4. Discussion

4.1. Morphological Examination of Copepod Specimens

The findings of this research underscore the imperative for targeted investigations focusing specifically on male specimens or females that have recently molted. Such a focused approach is essential for the delineation of definitive morphological characteristics, which, when clearly established, can be effectively integrated into molecular diagnostic protocols. This multifaceted methodology is expected to substantially enhance the accuracy and precision of species identification in future studies. Our investigation did not yield significant diagnostic markers that could facilitate a refined diagnosis at the genus level, a limitation stemming from the currently inadequate detail in the existing genus descriptions [14,17,19]. Furthermore, the study revealed an absence of significant morphological variation among specimens from different Caribbean regions. This observation could largely be attributed to the extensive morphological variability inherent in the female specimens of the genus, particularly noted in the reduction in appendages and the challenges in preserving structural details during gall dissection and analysis.

The significant taxonomic ambiguity of the Lamippidae family, primarily due to the absence of distinct morphological features for reliable species differentiation, is a well-documented challenge in the scientific community [14]. Our research underscores the necessity of detailed specimen analysis, emphasizing the inclusion of both male and female specimens for accurate species identification. This is crucial given the notable morphological diversity observed between the different genders and developmental stages within species, adding complexity to establishing definitive diagnostic characters for species delineation. To address these taxonomic challenges effectively and enhance genus-level diagnoses within the Lamippidae family, we advocate a dual-methodological approach, combining molecular techniques with detailed morphological analyses. This strategy aims to achieve a more refined and comprehensive taxonomic classification for the family, resolving existing taxonomic complexities and deepening our understanding of the phylogenetic and evolutionary relationships in this diverse and underexplored group of copepods.

Our observation of the dissolution of all copepod exuviae during the DNA extraction process suggests a potential weakening of the chitinous layer in these copepods. This finding deviates from the expected results based on previous studies that successfully conserved copepod exoskeletons [25,48,49]. Possible explanations for this phenomenon include a thinned chitin exoskeleton, characteristic of endoparasitic adaptations, or an altered chemical composition of the exoskeleton in Lamippidae copepods. The substitution of chitin with a more elastic protein, such as resilin, is another speculative explanation [50]. This unexpected result prompts the need for further in-depth examination of the exoskeletal structure of these unique copepods.

4.2. Molecular Phylogenetic Divergence

This study delineated copepod populations associated with the octocoral genus *Gorgonia* into three distinct phylogenetic clades, each endemic to specific geographic areas within the Caribbean. These clades are well supported and genetically distant enough to warrant the recognition of three novel, hitherto undescribed *Sphaerippe* species. These findings, particularly the values of Tajima's D and Fu's F statistics, imply a dynamic state of evolutionary flux within these populations, marked by an imbalance between genetic drift and mutations. The results are indicative of an extensive coevolutionary process between *Sphaerippe* copepods and their hosts. One clade, originating from the Eastern and Southern Caribbean marine ecoregions, predominantly inhabits the vicinity of the islands of St. Eustatius, Curaçao, and Bonaire, spanning approximately 900 km (Figure 1a). Notably, this clade exhibits minimal genetic variation over these considerable distances. The phylogeographic similarity between these different locations is not unique, since it can also be found in reef fishes [51,52]. This can be explained by a connectivity caused by the westward Caribbean Current from the Atlantic, entering the eastern Caribbean through the Lesser Antilles Arc and flowing towards the southern Caribbean [52].

Conversely, the western Caribbean clades show a distinct separation based on mitochondrial DNA sequences, with one subgroup associated with Cuba's southern coastline and the other with its northern counterpart. Intriguingly, analyses of nuclear internal transcribed spacer (ITS2) regions in these copepods have revealed genetic intermingling between some specimens from the southern clade with those from the northern clade, indicative of gene flow between these two distinct species. The occurrence of hybridization, particularly between *Sphaerippe* spp. from the disparate northern and southern Cuban coasts, suggests a lack of prezygotic morphological barriers to reproduction. This observation aligns with the hypothesis of larval dispersal facilitated by the currents of the Yucatan Strait, underscoring the significant influence of oceanographic factors on the evolutionary trajectory and geographic distribution of these Caribbean *Sphaerippe* species.

The taxonomic classification and determination of the phylogenetic order of copepods within the Lamippidae family, particularly considering their modified morphology and appendage reduction, has been long uncertain. These studies were complicated by the distinctive morphological traits of the Lamippidae, which historically led to their varied classification into orders such as Siphonostomatoida, Cyclopoida, and Poecilostomatoida [14]. Our phylogenetic analyses robustly place Lamippidae copepods, specialized endoparasites of octocorals (Octocorallia), within the order, Poecilostomatoida [14]. This research additionally revealed a sister relationship between Lamippidae and families of copepods known as symbionts of scleractinian corals (Anchimoligidae, Rhynchomolgidae, and Xarifidae). This phylogenetic arrangement not only underscores the evolutionary relationships within these taxa but also enhances the understanding of their systematic positions within the broader copepod lineage. Importantly, despite ongoing debates regarding the boundaries and validity of the orders, Cyclopoida and Poecilostomatoida, which have yet to be conclusively resolved through molecular methods, a significant group of predominantly symbiotic copepod families within these orders appeared to represent a cohesive and well-diagnosable group within our analyses [53–56]. This insight underlines the importance of continued molecular and morphological research to better understand the complexities of copepod taxonomy and their evolutionary relationships with various host taxa within marine ecosystems.

The *Gorgonia* sea fans analyzed in our study are characterized by a range of morphological variations in colony branching. This diversity was subject to much discussion on its taxonomic meaning until the advent of molecular methods for identifying interspecies boundaries among closely related groups (Figures S1–S7) [11,57,58]. Our genetic analyses revealed that the sequences of most *Gorgonia* taxa are congruent in both the ITS2 and msh1 markers. Furthermore, *Gorgonia* collectively form a monophyletic clade at the species level, which also includes sequences of *Gorgonia ventalina* and *G. flabellum*. This finding underscores the limitations of current DNA markers in effectively distinguishing the species within octocorals [59]. Given the impact of environmental factors on the morphological variability of corals [59,60], and considering the genetic homogeneity of our *Gorgonia* samples, we classified all specimens within the species *G. ventalina*. An outlier in our analysis was sample 19–32, which, based on the msh1 marker, was distinct in both Maximum Likelihood (ML) and Bayesian phylogenetic trees. Sequences from this specimen did not cluster with either those of our specimens or those in GenBank, suggesting it may represent a significantly divergent msh1 haplotype. However, its concordance in ITS2 markers and general external morphology with other *Gorgonia* specimens indicates its probable affiliation with the same species as the rest of our specimens.

4.3. Geographical Heterogeneity of Parasite and Host Populations

In our study, we discerned a conspicuous disparity in the species differentiation of *Sphaerippe* among copepods across distinct Caribbean regions, accompanied by a comparatively restricted intraspecific variability in the composition of their host *Gorgonia* populations and other symbionts associated with the same host (Figures 3–5) [61,62]. This pattern appears to be influenced by the relatively limited dispersal capability of both *Sphaerippe*

and *Gorgonia*. Throughout our field research, it was recurrently noted that colonies afflicted with Multifocal Purple Spot Syndrome (MFPS) were often located in proximity to healthy sea fan colonies. This proximity may be indicative of the copepods' ability for self-infection within sea fan colonies and their active role in attracting dispersal stages to parts of the population already parasitized by these copepods.

Our hypothesis posits that the nauplii of *Sphaerippe* spp., which develop inside the gall, or their first copepodid stage, acting as a dispersal phase in many parasitic copepods, are responsible for rupturing the gall coverings. These nauplii then disseminate within the *Gorgonia* colony of the maternal gall and the infected host colony and may also spread to and infect adjacent sea fan colonies [63–66]. Contrasting with the copepods, the planktonic larvae of *Gorgonia* spp. probably exhibit a prolonged pelagic phase, suggesting a more effective dispersal capability [62] (Figure 2). The data obtained from our research corroborate findings from another Caribbean symbiont-host relationship involving the pea crab *Dissodactylus primitivus* Bouvier, 1917 and the sea urchin *Meoma ventricosa* (Lamarck, 1816) [67]. In this relationship, geographically separate populations of the symbiotic crab and a uniformity in the host population were observed [67], underscoring the complexity of symbiotic interactions in marine ecosystems.

4.4. Coral Diseases and the Multifocal Purple Spot Syndrome (MFPS)

Coral diseases, initially detected in the 1970s, are characterized by alterations in coral structures and functions, resulting from the intricate interplay among the corals, their environmental context, and various pathogenic agents [1,68–71]. With the advent of climate change, corals are increasingly subjected to physiological stressors, leading to compromised immune responses. This heightened vulnerability transforms previously innocuous agents into potential pathogens [21,49,71–73]. Research into coral pathologies is further complicated by the inaccessible nature of their habitats and the lack of universally accepted methodologies for diagnosing disease etiologies [74]. As a result, the majority of current literature on coral diseases primarily focuses on symptomatology, often omitting detailed etiological information [20,21,69,75].

The multifocal purple spot syndrome (MFPS), identified in the widely distributed and shallow-water coral species *Gorgonia ventalina* in the Caribbean in 2005 [9], is characterized by the presence of multiple purple swellings or galls on the octocoral colony. These galls are distinctively devoid of any openings [12]. Research into the pathology of these conspicuous galls has implicated organisms from the Labyrinthulomycetes group, particularly the genera, *Aplanochytrium* and *Thraustochytrium* [7,74]. However, a more detailed anatomical investigation of *G. ventalina* specimens affected by MFPS revealed the presence of copepods from the genus *Sphaerippe*. Notably, galls that lacked external openings contained female copepods, occasionally with males, as well as numerous embryos, developing nauplii, and sizeable spermatophores ([12,49], present observations). This new insight into the condition has introduced a nuanced perspective on the etiological factors of MFPS, complicating the accurate diagnosis and characterization of the syndrome in this widespread, shallow-water coral species in the Caribbean ([1,71,76], present observations).

The etiological investigation of Multifocal Purple Spot Syndrome (MFPS) in *Gorgonia ventalina* necessitates a comprehensive experimental framework to elucidate the pathogenicity of coral-associated microorganisms. This approach is essential due to the current reliance on indirect evidence. A salient diagnostic characteristic of MFPS caused by the *Sphaerippe* copepods is the specific size and morphology of the lesions, signifying an initial immunological response of *Gorgonia* species aimed at mitigating pathogen proliferation. This response is evidenced by a change in the coloration of *Gorgonia* surface tissues, characterized by an abundance of purple sclerites, as reported in multiple studies [1,12,49,71,74,77]. Notably, the lesions associated with MFPS, typically small with smooth edges, are markedly distinct from other forms of lesions that are larger, irregular in shape, and exhibit purple coloring at the edges, as commonly observed in sea fans [78].

Furthermore, the spatial distribution of MFPS, governed by the transmission dynamics of the pathogen, requires further detailed examination. Extensive observational data from dives across different regions of the Caribbean Sea indicate a higher prevalence of MFPS in shallower waters, correlating with the presence of *Sphaerippe* copepods. This finding is contrasted by the deeper distribution of the Labyrinthulomycetes genera *Aplanochytrium* and *Thraustochytrium*, which are associated with similar disease manifestations in La Parguera Natural Reserve of the southwest coast of Puerto Rico [74,76]. The contrasting features between MFPS and diseases induced by other organisms suggest that copepods of the genus *Sphaerippe* are likely the principal pathogens of MFPS.

With regard to the life cycle of *Sphaerippe* copepods, following coral infestation, both male and female copepods consume coral tissue and undergo significant morphological transformations. Females develop into a spherical form, while males assume a seed-like shape, contained within the coral gall. This gall environment facilitates their growth, molting, and reproduction, as well as the development of numerous nauplii. The prevailing hypothesis posits that the emergence of copepods into the external environment occurs during the late naupliar or early copepodid stages, often leading to the rupture of coral tissues. Dissections of various galls have revealed instances where, despite the absence of living copepods, the galls contained only their exuviae and spermatophores, encapsulated in a dense yellowish substance, presumably secreted by the coral cells. This observation suggests that the lifespan of the female copepod may limit the duration of gall formation. Additionally, dissections have shown that in some cases, galls are devoid of living copepods and contain only their exuviae, indicating that the manifestation period of galls is potentially constrained by the lifespan of the female copepod. The penetration of copepods into the coral and gall formation by the female likely occurs during a dispersive, immature stage of the copepod, either through the polyp or directly through the coral's covering. However, the precise mechanisms of this penetration and subsequent gall formation remain unexplored. Furthermore, the characteristics of the metamorphic development of both female and male specimens, which have been documented exclusively in galls harboring females and not universally across all such galls, continue to be an area that has not been thoroughly investigated.

The scarcity of prior documentation of the distinct purple lesions characteristic of Multifocal purple spot syndrome (MFPS) in the shallow-water sea fans of the extensively studied Caribbean basin could be attributed to an oversight in scientific focus on this specific symptom. Alternatively, this absence might be indicative of a relatively recent emergence of MFPS in the Caribbean region, possibly driven by climatic changes over the last 25 years [79]. Observational studies have noted a significant 34% increase in the proportion of infected *Gorgonia* colonies relative to healthy ones within a seven-year period following the disease's identification [1,21]. Given the observed peak in disease prevalence during summer months, it is reasonable to speculate that climatic shifts or coastal water pollution may play a role in the increased manifestation of MFPS, likely influenced by the presence of gall-inducing copepods [21,72].

The current literature delineates the distribution of MFPS, spanning depths of 3–20 m along the coasts of Florida, Mexico, and the islands of Puerto Rico, Grand Cayman, Curaçao, St. Eustatius, and Grenada [1,9,12,21,74,76,78]. However, our analysis of underwater photographs from the iNaturalist website [80] indicates a potentially broader spread of both *Gorgonia* and MFPS. Additionally, our data reveal the syndrome's presence in various regions of Cuba, and on the islands of Curaçao, Bonaire, and St. Eustatius (Figure 7, Table A7). There is a pressing need for more comprehensive data on the presence or absence of MFPS in other Caribbean regions, particularly given the current limited understanding of the syndrome's impact on the health of the host *Gorgonia* octocorals.

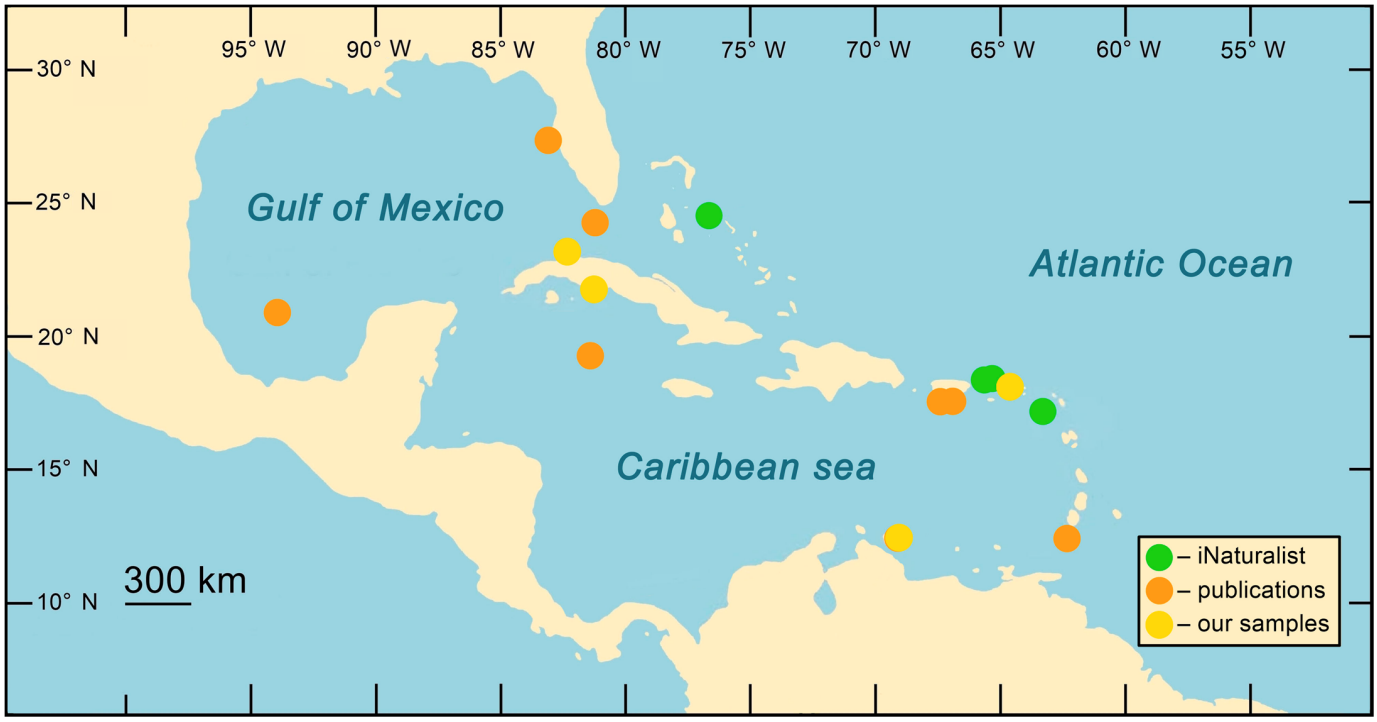

Figure 7. Localities of the multifocal purple spot syndrome (MFPS) records in the Caribbean Sea (see Table A7).

5. Conclusions

Gorgonia affected by MFPS and their associated gall-forming copepods, with their relatively straightforward diagnostic features, have the potential to become model organisms for research on shallow-water communities in the Caribbean. Their distinctive characteristics, conducive to identification and observation, provide valuable insights into the ecological dynamics and health of these ecosystems. By designating these corals and copepods as model systems, researchers will be able to gain profound insights into the interplay between corals and pathogens, the impact of environmental changes on marine biodiversity, and the mechanisms of disease spread and response in coral ecosystems. This knowledge is crucial for developing effective conservation and management strategies for these vital marine habitats. Additionally, the ease of identifying these organisms and the symptoms of MFPS renders them suitable for broader involvement in scientific studies, including by citizen scientists and SCUBA diving enthusiasts [81], thus popularizing scientific research and promoting a more inclusive approach to marine conservation.

Supplementary Materials: The following supporting information can be downloaded at: https://www.mdpi.com/article/10.3390/d16050280/s1, Figures S1–S10: Figure S1. Specimens of *Gorgonia ventalina* (Linnaeus 1758) labeled as follows: Statia15-99—1, 2; Statia15-134—3, 4; Statia15-135—5, 6; Statia15-141—7, 8. Figure S2. Specimens of *G. ventalina*. labeled as follows: Statia15-142—9, 10; Statia15-146—11, 12; Statia15-163—13, 14; Statia15-170—15, 16. Figure S3. Specimens of *G. ventalina* labeled as follows: Statia15-174—17, 18; CUR17-39—19, 20; CUR17-81—21, 22; CUR17-88—23, 24. Figure S4. Specimens of *G. ventalina* labeled as follows: CUR17-96—25, 26; Cuba19-1—27, 28; Cuba19-2—29, 30; Cuba19-3—31, 32. Figure S5. Specimens of *G. ventalina* labeled as follows: Cuba19-5—33, 34; Cuba19-21—35, 36; Cuba19-22—37; Cuba19-25—38, no; Cuba19-32—39, no; Cuba19-33—40. Figure S6. Specimens of *G. ventalina* labeled as follows: Cuba19-23—41, 42; Cuba19-27—43, 44; Cuba19-28—45, 46; Cuba19-30—47, 48. Figure S7. Specimens of *G. ventalina* labeled as follows: Bonaire19-28—50, 51; Bonaire19-31—52, 53; Bonaire19-47—54, 55; Bonaire19-91—56, 57. Figure S8. The phylogenetic tree was constructed based on the concatenated alignment of COI (Cytochrome c oxidase subunit I) and ITS2 (Internal Transcribed Spacer 2) sequences of Lamippidae copepods, including *Sphaerippe* spp. The model of nucleotide evolution is HKY + G for COI_pos1, K81UF + I for

ITS and COI_pos2, HKY + I for COI_pos3. The numbers in the nodes are posterior probabilities / bootstrap supports. The color bars on the right denote the species delimitation results. For additional details, including geographic coordinates, refer to Tables 1 and A4. Figure S9. In the Bayesian (BA) phylogenetic tree based on the alignment of 18S sequences of crustacean copepods, as indicated in Table A6, the nucleotide evolution model applied was GTR + G + I. The numbers associated with the nodes represent Bayesian (BA) posterior probabilities. For additional information, refer to Figure 6 and Supplementary Figure S10. Figure S10. Maximum Likelihood phylogenetic tree based on the 18S alignment of copepod crustaceans indicated in Table A6. The nucleotide evolution model applied is GTR + G + I. The numbers associated with the nodes represent bootstrap support values. For additional information, refer to Figure 6 and Supplementary Figure S9.

Author Contributions: Conceptualization and methodology, V.N.I., M.A.N. and B.W.H.; software, O.A.K. and M.A.N.; validation, O.A.K. and M.A.N.; formal analysis, O.A.K., V.N.I. and M.A.N.; dissection and microscopy, O.A.K. and V.N.I.; sampling, O.A.K., V.N.I., M.A., B.W.H. and J.D.R.; investigation, O.A.K., V.N.I., M.A.N., M.A., B.W.H. and J.D.R.; data curation, M.A.N., V.N.I. and O.A.K.; writing—original draft preparation, O.A.K., V.N.I. and M.A.N.; writing—review and editing, O.A.K., V.N.I., M.A.N., M.A., B.W.H. and J.D.R.; visualization, O.A.K., V.N.I. and M.A.N.; supervision, V.N.I.; project administration, V.N.I.; funding acquisition, V.N.I., M.A. and B.W.H. All authors have read and agreed to the published version of the manuscript.

Funding: This research was funded by the Russian Science Foundation Grant No. 22-24-00365.

Institutional Review Board Statement: Not applicable.

Data Availability Statement: See supplementary file with underwater photos of coral hosts of copepods and phylogenetic trees.

Acknowledgments: Our thanks also go to STINAPA Bonaire National Parks Foundation and the Dutch Caribbean Nature Alliance (DCNA) in Bonaire for their assistance with the research proposal submission and obtaining the necessary research permits. Additionally, V.N.I., B.W.H., and J.D.R. are thankful for the logistical support provided by STINAPA Bonaire, Dive Friends, and Budget Car Rental in Bonaire. The fieldwork conducted by V.N.I., J.D.R., and B.W.H. in St Eustatius received funding from the Martin and Temminck Fellowships at the Naturalis Biodiversity Center and was supported by St Eustatius Marine Parks (STENAPA), the Caribbean Netherlands Science Institute (CNSI), and the Scubaqua Dive Center. V.N.I., B.W.H., and J.D.R. also express their gratitude to the staff of CARMABI and the Dive Shop at Curaçao for their hospitality and logistic support. Fieldwork undertaken by O.A.K., M.A., and V.N.I. in Cuba was facilitated by funding from the RFBR–CITMA, adhering to both international and local regulations. Fieldwork in Dutch Caribbean was supported by Naturalis Biodiversity Center to V.N.I. and J.D.R. and by the WWF-Netherlands Biodiversity Fund to B.W.H. We extend our gratitude to the team of the Electron Microscopy Laboratory, Faculty of Biology, Lomonosov Moscow State University.

Conflicts of Interest: The authors declare no conflict of interest. The funder had no role in the design of the study; in the collection, analyses, or interpretation of data; in the writing of the manuscript; or in the decision to publish the results.

Appendix A

Table A1. List of primers used in molecular genetic analysis.

Gene	Primers	Primer Sequences (5′ to 3′)	References
ITS2 (coral)	5.8S-436	AGC ATG TCT GTC TGA GTG TTG G	[29]
ITS2 (coral)	28S-663	GGG TAA TCT TGC CTG ATC TGA G	[29]
msh1	ND42599	GCC ATT ATG GTT AAC TAT TAC	[30]
msh1	Mut-3458R	TSG AGC AAA AGC CAC TCC	[30]
ITS2 (copepod)	58dir-cop	CAG TGG ATC AYT TGG CTC GGG GG	[25]
ITS2 (copepod)	28r1-cop	CAT TCG CCA TTA CTA AGG GRA TCA C	[25]

Table A1. *Cont.*

Gene	Primers	Primer Sequences (5′ to 3′)	References
COI	LCO1490cop3	TCI TGI AAY CAY AAA GAY ATY GGI AC	[25]
COI	jgHCO2198	TAI ACY TCI GGR TGI CCR AAR AAY CA	[27]
18S	18d1	TGA AAC YGC GAA TGG CTC	A.V. Aleshin, unpublished
18S	18r3	CAA CTA CGA GCT TTT TAA C	A.V. Aleshin, unpublished
18S	Q39	GAA TGA TCC WTC YGC AGG TTC ACC TAC	[28]

Table A2. List of amplification temperature regimes for different primers.

Primers	Amplification Regime, Min	Amplified Fragments Lengths, bp
5.8S-436—28S-663 (coral)	1. 94 °C 02:00 2. 94 °C 00:30 3. 56 °C 00:45 4. 72 °C 00:45 5. 2 → 4 (38 cycles) 6. 72 °C 05:00	215–240
ND42599—Mut-3458R	1. 94 °C 02:00 2. 94 °C 00:30 3. 56 °C 00:45 4. 72 °C 00:45 5. 2 → 4 (38 cycles) 6. 72 °C 05:00	822–857
58dir-cop—28r1 (copepod)	1. 94 °C 02:00 2. 94 °C 00:20 3. 50 °C 00:20 4. 72 °C 01:00 5. 2 → 4 (38 cycles) 6. 72 °C 05:00	441–576
28d1—28r3	1. 94 °C 01:00 2. 94 °C 00:20 3. 55 °C 01:00 4. 72 °C 03:30 5. 2 → 4 (38 cycles) 6. 72 °C 10:00	657–667
LCO1490cop3—jgH2198	1. 94 °C 02:00 2. 94 °C 00:20 3. 45 °C 00:20 4. 72 °C 01:00 5. 2 → 4 (38 cycles) 6. 72 °C 05:00	617–687
18d1—Q39	1. 95 °C 03:00 2. 93 °C 00:20 3. 53 °C 00:20 4. 72 °C 01:30 5. 2 → 4 (40 cycles) 6. 72 °C 05:00	1537–1658

Table A3. GenBank accession numbers for ITS2 and msh1 sequences of coral specimens. For additional details, including geographic coordinates, please refer to Table 1.

Taxon	Specimen	Sample	ITS2	msh1
Gorgonia ventalina (Linnaeus 1758)	15-99	Statia15-99	OR977951	OR987860
	15-134	Statia15-134	OR977945	OR987862
	15-135	Statia15-135	OR977959	OR987863
	15-141	Statia15-141	OR977958	OR987864
	15-142	Statia15-142	OR977943	OR987865
	15-146	Statia15-146	OR977957	
	15-163	Statia15-163	OR977950	OR987872
	15-174	Statia15-174	OR977949	OR987858
	17-39	CUR17-39	OR977940	OR987859
	17-81	CUR17-81	OR977944	
	17-88	CUR17-88	OR977946	OR987873
	17-96	CUR17-96	OR977955	OR987866
	19-1	Cuba19-1	OR977956	
	19-3	Cuba19-3	OR977954	OR987867
	19-5	Cuba19-5	OR977942	OR987868
	19-22	Cuba19-22	OR977948	OR987861
	19-23	Cuba19-23	OR977941	OR987869
	19-25	Cuba19-25	OR977953	OR987870
	19-27	Cuba19-27	OR977952	OR987871
	19-28	Cuba19-28	OR977947	OR987857
	19-32	Cuba19-32		OR987874
	B28-4	Bonaire19-28		OR987876
	B31-4	Bonaire19-31		OR987877
	B47-4	Bonaire19-47		OR987875
	B91-4	Bonaire19-91	OR977951	OR987860

Table A4. GenBank accession numbers for 18S, COI, and ITS2 sequences of copepod specimens. For additional details, including geographic coordinates, refer to Table 1.

Taxon	Specimen	Sample	18S	COI	ITS2
Lamippidae	SLAVA122	AU-VI_1898	PP338814	PP330795	PP338815
	SLAVA123	AU-VI_1898		PP330796	PP338816
Sphaerippe spp.	K1	Statia15-170		PP330815	PP338838
	K2	Statia15-170		PP330816	PP338839
	K3	Statia15-170		PP330817	PP338840
	K4	Statia15-99			
	K5	Statia15-99		PP330818	PP338841
	K6	Statia15-99	PP338813	PP330819	PP338842
	O-1	CUR17-39		PP330828	PP338852
	O-2	CUR17-39		PP330834	PP338858
	O-3	CUR17-39		PP330835	PP338859
	O-4	CUR17-39		PP330836	PP338860
	O-5	CUR17-39		PP330837	PP338861
	O-6	CUR17-39		PP330838	PP338862
	O-7	CUR17-39		PP330839	PP338863
	O-8	Statia15-172		PP330840	
	O-9	Statia15-173		PP330841	PP338864
	O-10	Statia15-173		PP330820	PP338843
	O-11	Statia15-170		PP330821	PP338844
	O-12	Statia15-170			PP338845
	O-13	Statia15-170			PP338846
	O-14	Statia15-99		PP330822	PP338847
	O-15	Statia15-99		PP330823	PP338848
	O-16	Statia15-99		PP330824	PP338849

Table A4. *Cont.*

Taxon	Specimen	Sample	18S	COI	ITS2
	O-17	Statia15-99		PP330825	PP338850
	O-18	Statia15-141		PP330826	
	O-19	Statia15-141		PP330827	PP338851
	O-20	Statia15-141		PP330829	PP338853
	O-21	Statia15-142		PP330830	PP338854
	O-22	Statia15-142		PP330831	PP338855
	O-23	Statia15-142		PP330832	PP338856
	O-24	Statia15-142		PP330833	PP338857
	C-1	Cuba19-1			PP338827
	C-2	Cuba19-1			
	C-3	Cuba19-1		PP330797	PP338832
	C-4	Cuba19-2			PP338833
	C-5	Cuba19-3		PP330806	PP338834
	C-6	Cuba19-3		PP330807	PP338835
	C-7	Cuba19-3		PP330808	
	C-8	Cuba19-5		PP330813	PP338836
	C-9	Cuba19-5		PP330814	PP338837
	C-10	Cuba19-5			PP338817
	C-11	Cuba19-21		PP330798	PP338818
	C-12	Cuba19-5			PP338819
	C-13	Cuba19-23		PP330799	PP338820
	C-14	Cuba19-25		PP330800	PP338821
	C-15	Cuba19-25			PP338822
	C-16	Cuba19-25		PP330801	PP338823
	C-17	Cuba19-28		PP330803	PP338824
	C-18	Cuba19-28		PP330804	PP338825
	C-19	Cuba19-30		PP330809	PP338826
	C-20	Cuba19-33		PP330811	PP338828
	C-21	Cuba19-32		PP330810	PP338829
	C-22	Cuba19-27		PP330802	PP338830
	C-23	Cuba19-3		PP330805	PP338831
	C-24	Cuba19-5		PP330812	
	B28-1	Bonaire19-28			PP338867
	B28-2	Bonaire19-28		PP330794	PP338872
	B28-3	Bonaire19-28		PP330790	PP338871
	B31-1	Bonaire19-31		PP330786	PP338866
	B31-2	Bonaire19-31		PP330793	PP338865
	B31-3	Bonaire19-31		PP330791	PP338873
	B47-1	Bonaire19-47		PP330787	PP338868
	B47-2	Bonaire19-47		PP330789	
	B47-3	Bonaire19-47			
	B91-1	Bonaire19-91		PP330788	PP338869
	B91-2	Bonaire19-91			PP338870
	B91-3	Bonaire19-91		PP330792	

Table A5. GenBank accession numbers ITS2 and msh1 sequences of species used for phylogenetic analyses.

Scientific Name	ITS2	msh1
Gorgonia flabellum Bayer, 1961	AY587521	AY126427
Gorgonia mariae Bayer, 1961	AY587523	AY126426
Gorgonia ventalina (Linnaeus 1758)	AY587522	AY126425
Antillogorgia bipinnata (Verrill, 1864) (=*Pseudopterogorgia bipinnata* (Verrill, 1864))	AY126365	AY587524

Table A6. GenBank accession numbers 18S sequences of species used for phylogenetic analyses.

Order	Family	Scientific Name	18S
Cyclopoida		*Pachospunctatum*	GU969182
		Pachos sp.	AY627014
	Anchimolgidae	*Anchimolgidae* sp.	AY627000
		Anchimolgus sp.	AY627001
	Anthessiidae	*Anthessius* sp.	AY627002
	Archinotodelphyidae	*Archinotodelphys* sp.	JF781538
	Botryllophilidae	*Haplostoma kimi*	KR048722
	Cyclopettidae	*Paracyclopina nana*	FJ214952
	Cyclopidae	*Acanthocyclops viridis*	AY626999
		Apocyclops borneoensis	KR048733
		Apocyclops royi	AY626997
		Ectocyclops affinis	KR048732
		Ectocyclops polyspinosus	AJ746336
		Eucyclops serrulatus	AJ746328
		Eucyclops speratus	KR048717
		Euryte sp.	AY626996
		Cyclopidae sp.	AY210814
		Cyclops insignis	EF532821
		Cyclops kolensis	EF532820
		Cyclops sp.	AY626998
		Macrocyclops albidus	DQ538505
		Macrocyclops fuscus	KR048720
		Megacyclops viridis	KR048727
		Mesocyclops dissimilis	KR048719
		Mesocyclops pehpeiensis	KR048728
		Microcyclops varicans	KR048721
		Tropocyclops ishidai	KR048729
	Cyclopinidae	*Cyclopina gracilis*	JF781537
	Lernaeidae	*Lamproglena orientalis*	DQ107549
		Lernaea cyprinacea	DQ107554
	Mytilicolidae	*Mytilicola intestinalis*	AY627005
		Pectenophilus ornatus	AY627032
		Trochicola entericus	AY627006
	Notodelphyidae	*Bonnierilla curvicaudata*	KR048724
		Doropygus elegans	KR048723
		Doropygus rigidus	KR048730
		Notodelphys prasina	JF781536
		Pachypygus curvatus	KR048731
	Oithonidae	*Dioithona oculata*	KR048726
		Oithona similis	KR048725
		Oithona sp. 1	JF781539
		Oithona sp. 2	JF781540
	Rhynchomolgidae	*Doridicola agilis*	JF781541
		Critomolgus nudus	KR048760
		Critomolgus sp. 1	AY627008
		Critomolgus sp. 2	AY627009
		Critomolgus vicinus	KR048766
		Zamolgus cavernularius	KR048761
	Sabelliphilidae	*Sabelliphilidae* sp.	KR048767
		Sabelliphilus elongatus	AY627010
		Scambicornus sp.	AY627011
	Vahiniidae	*Vahinius* sp.	AY627012
	Xarifiidae	*Xarifia* sp.	AY627013
Misophrioida	Misophriidae	*Misophria* sp.	JF781533
		Misophriopsis okinawensis	JF781532
		Misophriopsis sp.	JF781534

Table A6. *Cont.*

Order	Family	Scientific Name	18S
Poecilostomatoida	Bomolochidae	*Holobomolochus* sp.	JF781551
		Nothobomolochus thambus	KR048747
	Catiniidae	*Catinia plana*	JF781555
		Catiniidae sp.	JF781554
	Chondracanthidae	*Acanthochondria spirigera*	KR048753
		Acanthochondria tchangi	KR048754
		Brachiochondria pinguis	KR048755
		Chondracanthus distortus	KR048756
		Chondracanthus zei	KR048770
		Lernentoma asellina	AY627003
	Clausidiidae	*Conchyliurus dispar*	KR048764
		Conchyliurus quintus.	KR048763
		Hemicyclops ctenidis.	KR048744
		Hemicyclops sp.	KT030266
		Hemicyclops tanakai	KR048769
		Hemicyclops thalassius	JF781552
	Clausocalanidae	*Clausia* sp.	KR048749
	Corycaeidae	*Corycaeus speciosus*	GU969165
	Ergasilidae	*Ergasilus tumidus*	DQ107569
		Ergasilus wilsoni	KR048765
		Neoergasilus japonicus	KR048752
		Sinergasilus undulatus	DQ107562
	Iveidae	*Ive* sp.	JF417992
	Lichomolgidae	*Astericola clausii*	JF781542
		Herrmannella longicaudata	KR048757
		Lichomolgus marginatus	JF781544
		Lichomolgus similis	KR048758
		Stellicola sp.	AY627004
	Myicolidae	*Ostrincola koe*	KR048750
		Pseudomyicola spinosus	KR048751
	Pseudanthessiidae	*Mecomerinx heterocentroti*	JF781545
		Pseudanthessius sp.	AY627007
	Sapphirinidae	*Copilia mirabilis*	GU969205
		Sapphirina scarlata	GU969208
	Synaptiphilidae	*Synaptiphilus longicaudus*	KR048745
	Taeniacanthidae	*Anchistrotos kojimensis*	KT030267
		Clausidium vancouverense	JF781553
		Clavisodalis abbreviatus	JF781549
		Irodes sauridi	JF781550
		Pseudotaeniacanthus congeri	KR048746
		Taeniacanthus kitamakura	JF781548
		Taeniacanthus yamagutii	KR048748
		Taeniacanthus zeugopteri	JF781547
		Umazuracola elongatus	JF781546

Table A7. List of multifocal purple spot syndrome (MFPS) geographic distributions with coordinates, depth data, and references (see Figures 1 and 7).

Host	Agent (in Source)	Higher Geography	Site	Geocoordinate	Accuracy (m)	Depth (m)	Month	Year	Source
Gorgonia ventalina	Protozoan (Labyrinthulomycote)	Florida	Florida	27.588099, −82.739206	320000			2005	[9,21]
Gorgonia ventalina	Protozoan (Labyrinthulomycote)	Mexico	Mexico	21.773321, −94.070358	390000			2005	[9,21]
Gorgonia ventalina and other octocorals	Protozoan (Labyrinthulomycote)	Puerto Rico	Puerto Rico	17.940083, −66.466573	100000	3–20		2005	[21,78]

Table A7. *Cont.*

Host	Agent (in Source)	Higher Geography	Site	Geocoordinate	Accuracy (m)	Depth (m)	Month	Year	Source
Gorgonia ventalina	*Aplanochytrium*	Puerto Rico	Media Luna	17.934883, −67.048850		3–18	July, September, October	2006–2010	[74]
Gorgonia ventalina	*Aplanochytrium*	Puerto Rico	Buoy	17.889667, −66.984833		18–25		2006–2010	[74]
Gorgonia ventalina	*Aplanochytrium*	Florida	Big Pine Ledges	24.553450, −81.378850			February	2010	[74]
Gorgonia ventalina	Labyrinthulid, Copepod	Puerto Rico	Turrumotico	17.929050, −66.974783			June, July	2013	[76]
Gorgonia ventalina	Labyrinthulid, Copepod	Puerto Rico	Turrumote	17.934950, −67.018833			June, July	2013	[76]
Gorgonia ventalina	Labyrinthulid, Copepod	Puerto Rico	Laurel Patch	17.942283, −67.067617			June, July	2013	[76]
Gorgonia ventalina	Labyrinthulid, Copepod	Puerto Rico	Media Luna	17.934933, −67.048517			June, July	2013	[76]
Gorgonia ventalina	Labyrinthulid, Copepod	Puerto Rico	Pelotas	17.957433, −67.069717			June, July	2013	[76]
Gorgonia ventalina	Labyrinthulid, Copepod	Puerto Rico	Caballo Blanco	17.963850, −67.049000			June, July	2013	[76]
Gorgonia ventalina	Labyrinthulid, Copepod	Puerto Rico	Enrique	17.954900, −67.043467			June, July	2013	[76]
Gorgonia ventalina	Labyrinthulid, Copepod	Puerto Rico	Corral Channel	17.949317, −66.998967			June, July	2013	[76]
Gorgonia ventalina	Labyrinthulid, Copepod	Puerto Rico	Fosfo Bay	17.959067, −67.013767			June, July	2013	[76]
Gorgonia ventalina	Labyrinthulid, Copepod	Puerto Rico	Mario reef	17.952833, −67.056450			June, July	2013	[76]
Gorgonia sp.	Labyrinthulid, Copepod	Grand Cayman	Grand Cayman	19.318796, −81.325228	15000				[1]
Gorgonia sp.	Labyrinthulid, Copepod	Curaçao	Curaçao	12.218792, −68.971464	33000				[1]
Gorgonia sp.	Labyrinthulid, Copepod	Grenada	Grenada	12.331716, −61.559601	30000				[1]
Gorgonia ventalina	Labyrinthulid, Copepod	Puerto Rico	La Parguera	17.964639, −67.051750	12000			2003–2012	[1]
Gorgonia ventalina	*Sphaerippe* sp. 1	St. Eustatius	Anchor Point North	17.463900, −62.987700		15–20	June	2015	This paper
Gorgonia ventalina	*Sphaerippe* sp. 1	St. Eustatius	Anchor Reef	17.462433, −62.985483		15.6	June	2015	This paper
Gorgonia ventalina	*Sphaerippe* sp. 1	St. Eustatius	Blund Shoal	17.464617, −62.977417		5.9	June	2015	This paper
Gorgonia ventalina	*Sphaerippe* sp. 1	St. Eustatius	English Quarter	17.505067, −62.962867		17.3	June	2015	This paper
Gorgonia ventalina	*Sphaerippe* sp. 1	St. Eustatius	Gallows Bay	17.475083, −62.986194		12	June	2015	This paper
Gorgonia ventalina	*Sphaerippe* sp. 1	St. Eustatius	Gibraltar	17.526817, −62.999300		5–20	June	2015	This paper
Gorgonia sp.	*Sphaerippe* sp. 1	St. Eustatius	The Blocks	17.464117, −62.985200		14.3	June	2015	This paper
Gorgonia ventalina	*Sphaerippe* sp. 1	St. Eustatius	Twin Sisters	17.516550, −63.003000		13.8	June	2015	This paper
Gorgonia sp.	*Sphaerippe* sp. 1	Curaçao	Buoy 1 (north of Piscadera Bay)	12.123056, −68.970556		8.2	June	2017	This paper
Gorgonia sp.	*Sphaerippe* sp. 1	Curaçao	Director's Bay	12.066389, −68.860556		4.1	June	2017	This paper
Gorgonia sp.	*Sphaerippe* sp. 1	Curaçao	Tugboat 2	12.068056, −68.862222		5.2–5.5	June	2017	This paper
Gorgonia sp.	*Sphaerippe* sp. 1	Curaçao	Playa Lagun	12.317222, −69.152500		4.9	June	2017	This paper
Gorgonia ventalina	*Sphaerippe* sp. 2	Cuba	Playa Salado	23.038981, −82.605153		4.5–8.5	February	2019	This paper
Gorgonia ventalina	*Sphaerippe* sp. 2	Cuba	Alejo el moro	22.115275, −81.116378		4.8–5.0	February	2019	This paper
Gorgonia ventalina	*Sphaerippe* sp. 3	Cuba	Centro de Investigaciones Marinas de la Universidad de La Habana	23.127431, −82.422689		8.1–11.6	February	2019	This paper
Gorgonia ventalina	*Sphaerippe* sp. 3	Cuba	Punta Perdiz	22.108236, −81.113728		8.3–13.8	February	2019	This paper
Gorgonia ventalina	Unknown	Virgin Islands	St. Thomas	18.335765, −64.896335	92000		October	2010	[80]
Gorgonia ventalina	Unknown	Puerto Rico	Playa Melones Culebra	18.304499, −65.311489	244		December	2013	[80]
Gorgonia ventalina	Unknown	Bahamas	Cape Eleuthera	24.812122, −76.343152	244		May	2019	[80]
Gorgonia ventalina	Unknown	St. Nevis	Jones Bay	17.196492, −62.613952			April	2017	[80]

References

1. Weil, E.; Rogers, C.S.; Croquer, A. Octocoral diseases in a changing ocean. In *Marine Animal Forests: The Ecology of Benthic Biodiversity Hotspots*; Rossi, S., Bramanti, L., Gori, A., Orejas Saco del Valle, C., Eds.; Springer International Publishing: Berlin/Heidelberg, Germany, 2017; pp. 1109–1163.
2. Calderón-Hernández, A.; Urbina-Villalobos, A.; Mora-Barboza, C.; Morales, J.A.; Fernández-García, C.; Cortés, J. Lesions in octocorals of the Costa Rican Caribbean During The 2015–2016 El Niño. *Coral Reefs* **2021**, *40*, 1167–1179. [CrossRef]
3. Becker, A.A.M.J.; Freeman, M.A.; Dennis, M.M. A combined diagnostic approach for the investigation of lesions resembling aspergillosis in Caribbean sea fans (*Gorgonia* spp.). *Veter. Pathol.* **2023**, *60*, 640–651. [CrossRef]
4. Knowlton, N.; Rohwer, F. Multispecies microbial mutualisms on coral reefs: The host as a habitat. *Am. Nat.* **2003**, *162*, 51–62. [CrossRef]
5. Ritchie, K.B. Regulation of microbial populations by mucus–associated bacteria. *Mar. Ecol. Prog. Ser.* **2006**, *322*, 1–14. [CrossRef]
6. Kimes, N.E.; Van Nostrand, J.D.; Weil, E.; Zhou, J.; Morris, P.J. Microbial functional structure of *Montastraea faveolata*, an important Caribbean reef–building coral, differs between healthy and Caribbean yellow–band diseased colonies. *Environ. Microbiol.* **2010**, *12*, 541–561. [CrossRef]
7. Burge, C.A.; Mouchka, M.E.; Harvell, C.D.; Roberts, S. Immune response of the Caribbean seafan, *Gorgonia ventalina* exposed to an *Aplanochytrium* parasite as revealed by transcriptome sequencing. *Front. Physiol.* **2013**, *4*, 180. [CrossRef]
8. Smith, G.W.; Weil, E. Aspergillosis of gorgonians. In *Coral Health and Disease*; Rosenberg, E., Loya, Y., Eds.; Springer: New York, NY, USA, 2004; pp. 270–286.
9. Harvell, C.D.; Markel, S.; Jordan-Dahlgren, E.; Raymundo, L.J.; Rosenberg, E.; Smith, G.W.; Willis, B.L.; Weil, E. Coral disease, environmental drivers and the balance between coral and microbial associates. *Oceanography* **2007**, *20*, 36–59. [CrossRef]
10. Ruiz-Moreno, D.; Willis, B.L.; Page, A.C.; Weil, E.; Croquer, A.; Vargas-Angel, B.; Jordan-Garza, A.G.; Jordán-Dahlgren, E.; Raymundo, L.; Harvell, C.D. Global coral disease prevalence associated with sea temperature anomalies and local factors. *Dis. Aquat. Org.* **2012**, *100*, 249–261. [CrossRef]
11. Bayer, F.M. The shallow–water *Octocorallia* of the West Indian region. *Stud. Fauna Curaçao Carib. Isl.* **1961**, *12*, 1–373.
12. Ivanenko, V.N.; Nikitin, M.A.; Hoeksema, B.W. Multiple purple spots in the Caribbean Sea fan *Gorgonia ventalina* caused by parasitic copepods at St. Eustatius, Dutch Caribbean. *Mar. Biodivers.* **2017**, *47*, 79–80.
13. Korzhavina, O.A.; Hoeksema, B.W.; Ivanenko, V.N. A review of Caribbean Copepoda associated with reef–dwelling cnidarians, echinoderms, and sponges. *Contrib. Zool.* **2019**, *88*, 297–349. [CrossRef]
14. Korzhavina, O.A.; Reimer, J.D.; Ehrlich, H.; Ivanenko, V.N. Global diversity and distribution of Lamippidae copepods symbiotic on Octocorallia. *Symbiosis* **2021**, *83*, 265–277. [CrossRef]
15. Korzhavina, O.A.; Grishina, D.Y.; Chen, X.; Fontaneto, D.; Ivanenko, V.N. Diving into diversity: Copepod crustaceans in octocoral association. *Diversity* **2023**, *15*, 1140. [CrossRef]
16. Humes, A.G. *Lamippe concinna* sp. n., a copepod parasitic in a West African pennatulid coelenterate. *Parasitology* **1957**, *47*, 447–451.
17. Grygier, M.J. Two new lamippid copepods parasitic on gorgonians from Hawaii and the Bahamas. *Proc. Biol. Soc. Wash.* **1980**, *93*, 662–673.
18. Grygier, M.J. An endoparasitic Lamippid Copepod in *Acanella* from the North Atlantic. *Crustaceana* **1983**, *45*, 176–182. [CrossRef]
19. Williams, J.D.; Anchaluisa, B.; Boyko, C.B.; McDaniel, N. Description of a new endoparasitic copepod genus and species (Lamippidae) that induces gall formation in leaves of the sea pen *Ptilosarcus gurneyi* (Octocorallia) from British Columbia. *Mar. Biodivers.* **2018**, *48*, 1325–1335. [CrossRef]
20. Weil, E. Coral reef diseases in the wider Caribbean. In *Coral Health and Disease*; Rosenberg, E., Loya, Y., Eds.; Springer: New York, NY, USA, 2004; pp. 35–68.
21. Weil, E.; Rogers, C.S. Coral reef diseases in the Atlantic–Caribbean. In *Coral Reefs: An Ecosystem in Transition*; Dubinsky, Z., Stambler, N., Eds.; Springer: Berlin/Heidelberg, Germany, 2011; pp. 465–491.
22. Kim, K.; Rypien, K. Aspergillosis of caribbean sea fan corals, *Gorgonia* spp. In *Diseases of Coral*; Woodley, C., Downs, C.A., Bruckner, A., Porter, J., Galloway, S.B., Eds.; Wiley: Hoboken, NJ, USA, 2015; pp. 236–241.
23. Hoeksema, B.W.; Reimer, J.D.; Vonk, R. Editorial: Biodiversity of Caribbean coral reefs (with a focus on the Dutch Caribbean). *Mar. Biodivers.* **2017**, *47*, 1–10. [CrossRef]
24. Ivanenko, V.N.; Defaye, D. A new and primitive genus and species of deep–sea Tegastidae (Crustacea, Copepoda, Harpacticoida) from the Mid–Atlantic Ridge, 37°N (Azores Triple Junction, Lucky Strike). *Cah. Biol. Mar.* **2004**, *45*, 255–268.
25. Ivanenko, V.N.; Hoeksema, B.W.; Mudrova, S.V.; Nikitin, M.A.; Martínez, A.; Rimskaya-Korsakova, N.N.; Berumen, M.L.; Fontaneto, D. Lack of host specificity of copepod crustaceans associated with mushroom corals in the Red Sea. *Mol. Phylogenetics Evol.* **2018**, *127*, 770–780. [CrossRef]
26. Porco, D.; Rougerie, R.; Deharveng, L.; Hebert, P. Coupling non–destructive DNA extraction and voucher retrieval for small soft–bodied Arthropods in a high–throughput context: The example of *Collembola*. *Mol. Ecol. Resour.* **2010**, *10*, 942–945. [CrossRef]
27. Geller, J.; Meyer, C.; Parker, M.; Hawk, H. Redesign of PCR primers for mitochondrial cytochrome c oxidase subunit I for marine invertebrates and application in all–taxa biotic surveys. *Mol. Ecol. Resour.* **2013**, *13*, 851–861. [CrossRef]
28. Medlin, L.; Elwood, H.J.; Stickel, S.; Sogin, M.L. The characterization of enzymatically amplified eukaryotic 16S–like rRNA–coding regions. *Gene* **1988**, *71*, 491–499. [CrossRef]

29. Aguilar, C.; Sánchez, J.A. Phylogenetic hypotheses of gorgoniid octocorals according to ITS2 and their predicted RNA secondary structures. *Mol. Phylogenetics Evol.* **2007**, *43*, 774–786. [CrossRef]
30. Sánchez, J.A.; McFadden, C.S.; France, S.C.; Lasker, H.R. Molecular phylogenetic analyses of shallow–water Caribbean octocorals. *Mar. Biol.* **2003**, *142*, 975–987. [CrossRef]
31. Kearse, M.; Moir, R.; Wilson, A.; Stones–Havas, S.; Cheung, M.; Sturrock, S.; Drummond, A. Geneious Basic: An integrated and extendable desktop software platform for the organization and analysis of sequence data. *Bioinformatics* **2012**, *28*, 1647–1649. [CrossRef] [PubMed]
32. Altschul, S.F.; Gish, W.; Miller, W.; Myers, E.W.; Lipman, D.J. Basic local alignment search tool. *J. Mol. Biol.* **1990**, *215*, 403–410. [CrossRef] [PubMed]
33. Edgar, R.C. MUSCLE: Multiple sequence alignment with high accuracy and high throughput. *Nucleic Acids Res.* **2004**, *32*, 1792–1797. [CrossRef]
34. Kuraku, S.; Zmasek, C.M.; Nishimura, O.; Katoh, K. aLeaves facilitates on–demand exploration of metazoan gene family trees on MAFFT sequence alignment server with enhanced interactivity. *Nucleic Acids Res.* **2013**, *41*, W22–W28. [CrossRef]
35. Katoh, K.; Rozewicki, J.; Yamada, K.D. MAFFT online service: Multiple sequence alignment, interactive sequence choice and visualization. *Brief. Bioinform.* **2017**, *20*, 1160–1166. [CrossRef] [PubMed]
36. Guindon, S.; Dufayard, J.F.; Lefort, V.; Anisimova, M.; Hordijk, W.; Gascuel, O. New algorithms and methods to estimate maximum–likelihood phylogenies: Assessing the performance of PhyML 3.0. *Syst. Biol.* **2010**, *59*, 307–321. [CrossRef] [PubMed]
37. Lanfear, R.; Calcott, B.; Ho, S.Y.; Guindon, S. PartitionFinder: Combined selection of partitioning schemes and substitution models for phylogenetic analyses. *Mol. Biol. Evol.* **2012**, *29*, 1695–1701. [CrossRef]
38. Lanfear, R.; Frandsen, P.B.; Wright, A.M.; Senfeld, T.; Calcott, B. PartitionFinder 2: New methods for selecting partitioned models of evolution for molecular and morphological phylogenetic analyses. *Mol. Biol. Evol.* **2016**, *34*, 772–773. [CrossRef]
39. Ronquist, F.; Teslenko, M.; Van Der Mark, P.; Ayres, D.L.; Darling, A.; Höhna, S.; Larget, B.; Liu, L.; Suchard, M.A.; Huelsenbeck, J.P. MrBayes 3.2: Efficient Bayesian phylogenetic inference and model choice across a large model space. *Syst. Biol.* **2012**, *61*, 539–542. [CrossRef]
40. Rambaut, A.; Drummond, A.J.; Xie, D.; Baele, G.; Suchard, M.A. Posterior summarization in Bayesian phylogenetics using Tracer 1.7. *Syst. Biol.* **2018**, *67*, 901–904. [CrossRef] [PubMed]
41. Trifinopoulos, J.; Nguyen, L.T.; von Haeseler, A.; Minh, B.Q. W-IQ-TREE: A fast online phylogenetic tool for maximum likelihood analysis. *Nucleic Acids Res.* **2016**, *44*, W232–W235. [CrossRef]
42. Felsenstein, J. Phylogenies and the comparative method. *Am. Nat.* **1985**, *125*, 1–15. [CrossRef]
43. Fontaneto, D.; Flot, J.F.; Tang, C.Q. Guidelines for DNA taxonomy, with a focus on the meiofauna. *Mar. Biodivers.* **2015**, *45*, 433–451. [CrossRef]
44. Leigh, J.W.; Bryant, D. POPART: Full–feature software for haplotype network construction. *Methods Ecol. Evol.* **2015**, *6*, 1110–1116. [CrossRef]
45. Tajima, F. Statistical method for testing the neutral mutation hypothesis by DNA polymorphism. *Genetics* **1989**, *123*, 585–595. [CrossRef]
46. Ivanenko, V.N.; Corgosinho, P.H.; Ferrari, F.; Sarradin, P.M.; Sarrazin, J. Microhabitat distribution of Smacigastes micheli (Copepoda: Harpacticoida: Tegastidae) from deepsea hydrothermal vents at the Mid-Atlantic Ridge, 37° N (Lucky Strike), with a morphological description of its nauplius. *Marine Ecology* **2012**, *33*, 246–256. [CrossRef]
47. Fu, Y.-X. Statistical tests of neutrality against population growth, hitchhiking and background selection. *Genetics* **1997**, *147*, 915–925. [CrossRef]
48. Conradi, M.; Bandera, E.; Mudrova, S.V.; Ivanenko, V.N. Five new coexisting species of copepod crustaceans of the genus *Spaniomolgus* (Poecilostomatoida: Rhynchomolgidae), symbionts of the stony coral *Stylophora pistillata* (Scleractinia). *ZooKeys* **2018**, *791*, 71–95. [CrossRef]
49. Shelyakin, P.V.; Garushyants, S.K.; Nikitin, M.A.; Mudrova, S.V.; Berumen, M.; Speksnijder, A.G.C.L.; Hoeksema, B.W.; Fontaneto, D.; Gelfand, M.S.; Ivanenko, V.N. Microbiomes of gall–inducing copepod crustaceans from the corals *Stylophora pistillata* (Scleractinia) and *Gorgonia ventalina* (Alcyonacea). *Sci. Rep.* **2018**, *8*, 11563. [CrossRef]
50. Michels, J.; Appel, E.; Gorb, S.N. Functional diversity of resilin in Arthropoda. *Beilstein J. Nanotechnol.* **2016**, *7*, 1241–1259. [CrossRef] [PubMed]
51. Taylor, M.S.; Hellberg, M.E. Comparative phylogeography in a genus of coral reef fishes: Biogeographic and genetic concordance in the Caribbean. *Mol. Ecol.* **2006**, *15*, 695–707. [CrossRef] [PubMed]
52. Rocha, L.A.; Rocha, C.R.; Robertson, D.R.; Bowen, B.W. Comparative phylogeography of Atlantic reef fishes indicates both origin and accumulation of diversity in the Caribbean. *BMC Evol. Biol.* **2008**, *8*, 157. [CrossRef] [PubMed]
53. Huys, R.; Llewellyn-Hughes, J.; Olson, P.D.; Nagasawa, K. Small subunit rDNA and Bayesian inference reveal *Pectenophilus ornatus* (Copepoda incertae sedis) as highly transformed Mytilicolidae, and support assignment of Chondracanthidae and Xarifiidae to Lichomolgoidea (Cyclopoida). *Biol. J. Linn. Soc.* **2006**, *87*, 403–425. [CrossRef]
54. Ferrari, F.D.; Ivanenko, V.N.; Dahms, H.-U. Body architecture and relationships among basal copepods. *J. Crustac. Biol.* **2010**, *30*, 465–477. [CrossRef]
55. Mikhailov, K.V.; Ivanenko, V.N. Lack of reproducibility of molecular phylogenetic analysis of Cyclopoida. *Mol. Phylogenetics Evol.* **2019**, *139*, 106574. [CrossRef] [PubMed]

56. Mikhailov, K.V.; Ivanenko, V.N. Low support values and lack of reproducibility of molecular phylogenetic analysis of Copepoda orders. *Arthropoda Selecta* **2021**, *30*, 39–42. [CrossRef]
57. Sanchez, J.A.; Wirshing, H.H. A field key to the identification of tropical western Atlantic zooxanthellate octocorals (Octocorallia: Cnidaria). *Carib. J. Sci.* **2005**, *41*, 508–522.
58. McFadden, C.S.; France, S.C.; Sánchez, J.A.; Alderslade, P. A molecular phylogenetic analysis of the Octocorallia (Cnidaria: Anthozoa) based on mitochondrial protein–coding sequences. *Mol. Phylogenetics Evol.* **2006**, *41*, 513–527. [CrossRef]
59. McFadden, C.S.; Sánchez, J.A.; France, S.C. Molecular phylogenetic insights into the evolution of Octocorallia: A review. *Integr. Comp. Biol.* **2010**, *50*, 389–410. [CrossRef]
60. Sanchez, J.A.; Aguilar, C.; Dorado, D.; Manrique, N. Phenotypic plasticity and morphological integration in a marine modular invertebrate. *BMC Evol. Biol.* **2007**, *7*, 122. [CrossRef] [PubMed]
61. Andras, J.P.; Kirk, N.L.; Harvell, C.D. Range–wide population genetic structure of *Symbiodinium* associated with the Caribbean Sea fan coral, *Gorgonia ventalina*. *Mol. Ecol.* **2011**, *20*, 2525–2542. [CrossRef]
62. Andras, J.P.; Rypien, K.L.; Harvell, C.D. Range–wide population genetic structure of the Caribbean sea fan coral, *Gorgonia ventalina*. *Mol. Ecol.* **2013**, *22*, 56–73. [CrossRef]
63. Ivanenko, V.N.; Ferrari, F.D.; Smurov, A.V. Nauplii and copepodids of *Scottomyzon gibberum* (Copepoda: Siphonostomatoida: Scottomyzotidae, a new family), a symbiont of *Asterias rubens* (Asteroidea). *Proc. Biol. Soc. Wash.* **2001**, *114*, 237–261.
64. Ivanenko, V.N.; Ferrari, F.D. Redescription of adults and description of copepodid development of *Dermatomyzon nigripes* (Brady, Robertson, 1876) and of *Asterocheres lilljeborgi* Boeck, 1859 (Copepoda: Siphonostomatoida: Asterocheridae). *Proc. Biol. Soc. Wash.* **2003**, *116*, 661–691.
65. Cheng, Y.R.; Lin, C.Y.; Yu, J.K. Embryonic and post–embryonic development in the parasitic copepod *Ive ptychoderae* (Copepoda: Iviidae): Insights into its phylogenetic position. *PLoS ONE* **2023**, *18*, e0281013. [CrossRef]
66. Williams, E.H., Jr.; Bunkley-Williams, L. Life cycle and life history strategies of parasitic Crustacea. *Parasit. Crustac.* **2019**, *3*, 179–266.
67. Jossart, Q.; De Ridder, C.; Lessios, H.A.; Bauwens, M.; Sébastien, M.; Thierry, R.; Rémi, A.W.; Bruno, D. Highly contrasted population genetic structures in a host–parasite pair in the Caribbean Sea. *Ecol. Evol.* **2017**, *7*, 9267–9280. [CrossRef]
68. Martin, S.W.; Meek, A.H.; Willerberg, P. *Veterinary Epidemiology, Principles and Methods*; Iowa State University Press: Ames, IA, USA, 1987; p. 343.
69. Work, T.M.; Aeby, G.S. Systematically describing gross lesions in corals. *Dis. Aquat. Org.* **2006**, *70*, 155–160. [CrossRef]
70. Rogers, C.S. Words matter: Recommendations for clarifying coral disease nomenclature and terminology. *Dis. Aquat. Org.* **2010**, *91*, 167–175. [CrossRef]
71. van de Water, J.A.J.M.; Allemand, D.; Ferrier-Pagès, C. Host–microbe interactions in octocoral holobionts—Recent advances and perspectives. *Microbiome* **2018**, *6*, 64. [CrossRef] [PubMed]
72. Rosenberg, E.; Ben-Haim, Y. Microbial diseases of corals and global warming. *Environ. Microbiol.* **2002**, *4*, 318–326. [CrossRef] [PubMed]
73. Lesser, M.P.; Bythell, J.C.; Gates, R.D.; Johnstone, R.W.; Hoegh–Guldberg, O. Are infectious diseases really killing corals? Alternative interpretations of the experimental and ecological data. *J. Exp. Mar. Biol. Ecol.* **2007**, *346*, 36–44. [CrossRef]
74. Burge, C.A.; Douglas, N.; Conti-Jerpe, I.; Weil, E.; Roberts, S.; Friedman, C.S.; Harvell, C.D. Friend or foe: The association of Labyrinthulomycetes with the Caribbean sea fan *Gorgonia ventalina*. *Dis. Aquat. Org.* **2012**, *101*, 1–12. [CrossRef] [PubMed]
75. Montano, S.; Maggioni, D.; Liguori, G.; Arrigoni, R.; Berumen, M.L.; Seveso, D.; Galli, P.; Hoeksema, B.W. Morpho–molecular traits of Indo–Pacific and Caribbean *Halofolliculina* ciliate infections. *Coral Reefs* **2020**, *39*, 375–386. [CrossRef]
76. Tracy, A.M.; Weil, E.; Harvell, C.D. Octocoral co–infection as a balance between host immunity and host environment. *Oecologia* **2018**, *186*, 743. [CrossRef] [PubMed]
77. Petes, L.E.; Harvell, C.D.; Peters, E.C.; Webb, M.A.H.; Mullen, K.M. Pathogens compromise reproduction and induce melanization in Caribbean Sea fans. *Mar. Ecol. Prog. Ser.* **2003**, *264*, 167–171. [CrossRef]
78. Weil, E.; Hooten, A.J. *Underwater Cards for Assessing Coral Health on Caribbean Reefs*; GEF–CRTR Program, Center for Marine Sciences, University of Queensland: Brisbane, Australia, 2008.
79. Chollett, I.; Müller-Karger, F.E.; Heron, S.F.; Skirving, W.; Mumby, P.J. Seasonal and spatial heterogeneity of recent sea surface temperature trends in the Caribbean Sea and southeast Gulf of Mexico. *Mar. Pollut. Bull.* **2012**, *64*, 956–965. [CrossRef]
80. iNaturalist. Available online: https://www.inaturalist.org (accessed on 15 December 2022).
81. Korein, E.; Vega-Rodriguez, M.; Metz Estrella, T. Developing recommendations for coral disease management in Puerto Rico using key informant interviews and participatory mapping. *Ocean Coast. Manag.* **2023**, *236*, 106488. [CrossRef]